universität wien

MASTERARBEIT / MASTER'S THESIS

Titel der Masterarbeit / Title of the Master's Thesis

„Impact of mTORC2 on mitochondrial physiology and M2 polarization in macrophages"

verfasst von / submitted by

Martin Hirtl, BSc

angestrebter akademischer Grad / in partial fulfilment of the requirements for the degree of

Master of Science (MSc)

Wien, 2018 / Vienna 2018

Studienkennzahl lt. Studienblatt / degree programme code as it appears on the student record sheet:	A 066 834
Studienrichtung lt. Studienblatt / degree programme as it appears on the student record sheet:	Masterstudium Molekulare Biologie
Betreut von / Supervisor:	Assoc.Prof. Dr. Thomas Weichhart

Acknowledgements

First of all I would like to thank my thesis advisor Thomas Weichhart of the Institute of Medical Genetics at the Medical University of Vienna for the opportunity to work on my thesis in his research group, his input, support and patience to see the work through.

I would also like to thank Karl Katholnig for the countless hours of discussion and when we worked together in the lab on different aspects of our Rictor$^{\Delta M}$ macrophages. I am grateful the provided support of everyone else from the Weichhart and Dolznig Groups and also to everyone else in the Institute of Medical Genetics, it was great sharing laboratory with all of you during one and a half years.

A special thanks goes out to all my friends who morally supported me the past years, you know who you are !

Finally, I must express a very special gratitude to my parents and family, who supported me from beginning to end and showed immense patience with me. Thank you all.

Martin

Прощай Просперо

Contents

List of Figures ii

List of Tables ii

1 Introduction 1

1.1 Innate immune system 1

1.1.1 Macrophages 2

1.2 Mechanistic target of rapamycin 3

1.3 Mouse model 5

2 Aim of the study 7

3 Materials and methods 8

3.1 Buffers, media, solutions 8

3.2 Methods 11

3.2.1 Western Blot 11

3.2.2 Bone marrow extraction 12

3.2.3 Peritoneal macrophage extraction 13

3.2.4 Generation of bone marrow-derived macrophages 13

3.2.5 Scratch assay 14

3.2.6 Annexin V - PI Apoptosis assay 14

3.2.7 Cell cycle analysis 14

3.2.8 Cell cycle analysis with peritoneal macrophages 14

3.2.9 2-NBDG uptake 15

3.2.10 2-NBDG uptake with peritoneal macrophages 15

3.2.11 Mitotracker Green FM 15

3.2.12 Mitotracker Red CMX Ros 16

3.2.13 Antibodies and dyes used in flow cytometry 16

4 Results 17

4.1 Deletion of Rictor abrogates Akt phosphorylation at Ser473 17

4.2 No significant difference in wound healing 18

4.3 Increased apoptosis of Rictor$^{\Delta M}$ macrophages during prolonged nutrient deprivation . . . 19
4.4 Loss of Rictor leads to cell cycle lag in macrophages . . . 20
4.5 mTORC2 controls glucose uptake . . . 22
4.6 Rictor$^{\Delta M}$ macrophages exhibit diminished mitochondrial membrane potential and elevated ER-stress . . . 24

5 Discussion **27**

References **33**

List of Figures

1.1 Overview of mTOR pathways . . . 4
1.2 Conditional deletion of Rictor in a mouse model . . . 6

4.1 Immunoblot analysis of mTORC2 downstream targets . . . 17
4.2 Scratch assay with no difference in wound healing ability . . . 18
4.3 Higher apoptosis rate of Rictor$^{\Delta M}$ macrophages after nutrient starvation of 48h . . . 19
4.4 Cell cycle lag of Rictor$^{\Delta M}$ bone marrow-derived macrophages . . . 20
4.5 Cell cycle lag of Rictor$^{\Delta M}$ peritoneal macrophages . . . 21
4.6 Immunoblot analysis of p27(KIP1) and p-Rb after FCS stimulation . 21
4.7 q-PCR of M1 and M2 marker proteins . . . 22
4.8 Diminished glucose uptake in LPS and IL-4 stimulated Rictor$^{\Delta M}$ macrophages . . . 23
4.9 Arg-1 expression lowered to the same as Rictor$^{\Delta M}$ macrophages after IL-4 and 2-DG stimulation . . . 24
4.10 Differences in mitochondrial mass and membrane potential . . . 25
4.11 Elevated levels of ER stress marker proteins in Rictor$^{\Delta M}$ macrophages 26

5.1 Impact of mTORC2 on M2 polarization . . . 31

List of Tables

3.1 Compounds of stacking and resolution gels used in SDS-PAGE 11
3.2 Antibodies used for Western Blot 12
3.3 Antibodies and dyes used in flow cytometry 16

Abstract

The role of the mechanistic target of rapamycin complex 1 (mTORC1) in macrophage activation and metabolism is well characterized, whereas the impact of mTOR complex 2 (mTORC2) on macrophage activation and metabolism remains poorly understood. Recent studies have shown that loss of Rictor, a key component of mTORC2, leads to a hyperinflammatory phenotype in macrophages if challenged with TLR ligands and to high expression levels of M1 marker genes and diminished expression of M2 marker genes.

To explore the significance of mTORC2 in macrophage metabolism we evaluated wound healing ability, apoptosis rate, cell cycle progression, glucose uptake, mitochondrial mass and mitochondrial membrane potential ($\Delta\Psi$) of mouse macrophages that had Rictor conditionally deleted (Rictor$^{\Delta M}$).

Our data showed no significant difference in wound healing, but increased apoptosis after 3 days of serum deprivation and a distinct lag in G1 to S phase progression probably due to decreased Akt-mediated phosphorylation of Rb in Rictor$^{\Delta M}$ macrophages. Moreover Rictor deletion led to a decreased glucose uptake after either LPS or IL-4 stimulation and also decreased $\Delta\Psi$.

Interestingly upon IL-4 stimulation of macrophages, the glycolytic inhibitor 2-DG was able to decrease the expression of M2 marker gene Arg1 in control macrophages to the same extent as observed in untreated Rictor deficient macrophages and 2-DG also could not further downregulate Arg1 expression in Rictor$^{\Delta M}$ macrophages. Furthermore upon treatment of Rictor$^{\Delta M}$ and control macrophages with thapsigargin, an intracellular calcium releaser, the $\Delta\Psi$ of control macrophages was lowered to the same levels as Rictor$^{\Delta M}$ macrophages. Additionally we discerned increased levels of unfolded protein response (UPR) marker proteins GRP78 and GADD135/CHOP in Rictor$^{\Delta M}$ macrophages.

Together our data shows that mTORC2 controls M2 polarization in macrophages, is a key part in coordinating glucose uptake and mitochondrial function and that glycolysis controls M2 polarization. The results also hint at the important role of mTORC2 in alleviating ER stress in macrophages.

Zusammenfassung

Die Rolle vom mechanistischen Ziel von Rapamycin - Komplex 1 (mTORC1) bei der Aktivierung und beim Metabolismus von Makrophagen ist sehr gut bekannt, jedoch der Einfluss von mTOR Komplex 2 (mTORC2) auf die Aktivierung und den Metabolismus von Makrophagen ist noch nicht so gut erforscht. In den letzten Jahren wurden Studien bekannt, welche zeigten, dass der Verlust von Rictor, ein essentieller Teil der mTORC2 Kinase, zu einem hyperinflammatorischen Phänotyp in Makrophagen führt, wenn sie mit TLR Liganden stimuliert werden.
Um die Singifikantz von mTORC2 in Makrophagen zu charakterisieren, analysierten wir die Wundheilungseigenschaft, Apoptosisrate, Zellzyklus Progression, Glukose Aufnahme, mitochondriale Masse und mitochondriales Membranenpotential ($\Delta\Psi$) in mäuslichen Makrophagen, bei welchen Rictor genetisch gelöscht wurde (Rictor$^{\Delta M}$). Unsere Daten zeigen keinen signifikanten Unterschied in der Wundheilung, aber nach 3 Tagen Nahrungsentzug erhöhtes Zellsterben und eine, wahrscheinlich aufgrund der fehlenden Phosphorylierung von Rb durch Akt, Verzögerung in der G1 zu S Phase Passage in Rictor$^{\Delta M}$ Makrophagen. Weiters führte der Verlust von Rictor auch zu einer niedrigen Glukose Aufnahme, wenn die Makrophagen mit LPS oder IL-4 stimuliert wurden und zu einem verringerten $\Delta\Psi$.
Interessanterweise konnte bei Stimulation von Kontrollmakrophagen durch IL-4, die Expression des M2 Markergens Arg1 durch Zugabe des Glykolyse Inhibitors 2-DG in der selben Weise gesenkt werden, wie wir es bei nicht behandelten Rictor$^{\Delta M}$ Makrophagen beobachten konnten. Auch konnte Zugabe von 2-DG zu IL-4 stimulierten Rictor$^{\Delta M}$ Makrophagen die Expression des Arg1 Gens nicht weiter zurück regulieren.
Zusätzlich konnte auch das $\Delta\Psi$ von Kontrollmakrophagen durch das Einwirken des intrazellulären Kalziumfreisetzers Thapsigargin auf das Level von Rictor$^{\Delta M}$ Makrophagen angeglichen werden und wir fanden erhöhte Mengen der UPR Markerproteine GRP78 und GADD135/CHOP in Rictor$^{\Delta M}$.
Zusammengefasst zeigen unsere Daten, dass mTORC2 in Makrophagen die M2 Polarisation kontrolliert, eine wichtige Rolle in der Koordination der Glukoseaufnahme und mitochondrialen Funktion spielt und dass Glykolyse auch die M2 Polarisation kontrolliert. Weiters weisen die Ergebnisse darauf hin, dass mTORC2 auch wichtig für das Erleichtern des ER Stresses in Makrophagen ist.

1. Introduction

1.1 Innate immune system

The innate immune system is the well preserved primary line of defense a host brings to bear against invading pathogenic infectious agents. Foremost, this protection is achieved through epithelial barriers warding the host against pathogens. The next line consists of the complement system and effector cells identifying threats, followed by effector cell-expressed cytokines [1]. After the initial recognition of pathogens, the innate immune system triggers the adaptive immunity in order to launch a full immune system activation.
Conserved pathogen-associated molecular patterns (PAMPs) of pathogens or danger-associated molecular patterns (DAMPs) are recognized by various innate immune system cells through various pattern recognition receptors (PRRs) [2]. These PRRs are located in various cell types, on the cell surface, in endocytic compartments and in the cytoplasm, and among them are Toll-like receptors (TLRs), RIG-I-like receptors (RLRs), NOD-like receptors (NLRs) and C-type lectin receptors (CLRs). The recognition of these PAMPs by PRRs activate complex signaling pathways, which lead to the onset of inflammation by the expression of various transcription factors, adaptor molecules, cytokines and chemokines.

For example if the plasma membrane localized TLR-4 recognizes lipopolysaccaride (LPS), then the adaptor molecules MyD88, TRIF, TIRAP and TRAM are recruited to the TIR-domain of TLR-4. This incites the downstream stimulation of NF$\varkappa$B, MAP kinase and IRF3, which induce the production of type 1 interferones and inflammatory cytokines [3], which in turn activates other monocytes, macrophages and dendritic cells. Upon recognition of a pathogen or opsonized particles by neutrophiles or macrophages expressing cell surface Fc receptors and additional ligation of PRRs by either PAMPs or DAMPs, various signal cascades are activated to initiate phagocytosis [4, 5]. Subsequently, the plasma membrane forms a phagosome by incapsulating the pathogen into a vesicle. Afterwards the phagosome and a lysosome fuse to form a phagolysosome in order to neutralize the phagocytosed pathogen by application of nitric oxide (NO) and reactive oxygen species (ROS). These phagocytes then continue to ripe into antigen presenting cells (APCs). Following which the APCs display the antigen peptides in either major histocompitability complex (MHC) I for CD8+ T cells or MHC II for CD4+ T cells [6, 7] in order to bridge the gap from innate to adaptive immunity and achieve a complete immune system activation.

1.1.1 Macrophages

As a key cell type in the innate immune system macrophages reside throughout the body as auxiliaries to most tissues. These tissue resident macrophages are labeled differently depending on their location. For example microglia in the central nervous system, Kupffer cells in the liver and osteoclasts in the bones. Although these macrophage subsets display different transcriptional profiles, morphology and phenotypes, most of them share the same haematopoietic progenitor, their main function as professional phagocytes, their role in immune response to pathogenes and tissue homeostasis [8]. In newborns the tissue resident macrophages proliferate in situ in abundance, following a reduced proliferation rate in adults for homeostatic purposes. These tissue resident macrophages play an important role after the inflammatory response in replenishing the number of resident macrophages via a proliferative burst [9]. During acute inflammation macrophage numbers are raised by in situ proliferation of tissue resident macrophages and later by patrolling monocytes which are recruited to the origin of the pathogen derived signals by chemokines and differentiate into additional macrophages. Through their PRRs macrophages are able to recognize microbes and are polarized toward an M1 inflammatory phenotype.

LPS and INFγ induced M1 polarization in macrophages leads to a change in macrophage metabolism, where the primary energy source is glycolysis instead of oxidative phosphorylation (OXPHOS). A key difference of these M1 and M2-polarized metabolic states is that in M1 macrophages arginine is used as substrate for inducible nitric oxide synthase (iNOS) to generate NO, which leads to an inhibition of mitochondrial metabolism and consequently making iNOS a prominent marker for M1 polarization. This NO-mediated inhibition of mitochondrial metabolism reduces mitochondrial respiration in favor of generating ROS which, alongside nicotinamide adenine dinucleotide phosphate (NADPH) oxidase produced ROS, are utilized for killing off phagocytosed bacteria and microbicidal activity.

TLR stimulation also activates the mechanistic target of rapamycin complex 1 (mTORC1) and this serine/threonine protein kinase in turn increases, among other downstream targets, the expression of transcription factor hypoxia-inducible factor 1α (HIF-1α). HIF-1α enhances the expression of inflammatory genes and the metabolic switch towards glycolysis through increased expression of pyruvate dehydrogenase kinase, which inhibits the conversion of pyruvate to acetyl CoA for the tricarboxylic acid (TCA) cycle. Also the expression and surface translocation of glucose transporter 1 (GLUT1) is amplified [10, 11].

These M1 macrophages initiate phagocytosis and secrete additional inflammatory cytokines such as TNFα, IL-1, IL-6, IL-8 and IL-12. Endogenous pyrogens IL-1

and IL-6 act as chemoattractant for granulocytes, promote the hepatic production of acute phase proteins and augment the expression of cell adhesion molecules on endothelial cells and leukocytes. IL-12 stimulates Th1 cells to produce INFγ, which in concert with TNFα heightens the activation of macrophages. M1-polarized macrophages are generally associated with inflammation, Th1 responses, tumor suppression and antimicrobial properties.

In contrast to M1, M2 macrophages are linked to Th2 responses, tissue homeostasis, wound healing, parasite clearance, immunosuppression and tumor promotion. IL-4 and IL-13 exposure leads to M2 polatization and these M2 macrophages lean heavily on oxidative phosphorylation, fatty acid oxidation and mitochondrial respiration for energy production. This switch towards an oxidative metabolism is mediated through IL-4 and IL-13 activation of TSC1 and TSC2, which inhibit mTORC1 activity and this in turn leads to reduced expression of HIF-1α. In M2-polarized macrophages arginine is used as a substrate for arginase 1 (ARG1) instead of iNOS, making ARG1 one of the prominent markers for M2 polarization. The immunosuppressive function of M2 macrophages is achieved by the release of the anti inflammatory cytokines IL-10 and transforming growth factor beta (TGF-β), which attenuate the microbicidal activity and INFγ-mediated activation of macrophages. Furthermore IL-10 is a powerful suppressor of MHC II expression and also inhibits the INFγ distribution of Th1 and NK cells.

Through different activation stimuli from the micro environment macrophages are able to adapt their metabolism to respond in a distinct and currently required manner. It is important to note that M1 and M2 describe extreme stages of macrophage polarization and in vivo more variants in between exist [12–14].

1.2 Mechanistic target of rapamycin

The mechanistic target of rapamycin (mTOR) is the central component in two fundamentally distinct kinase complexes, which play a major role in myriad vital cell functions. These kinase complexes are distinguished by their different components, regulatory-associated protein of mTOR (Raptor) in mTORC1 and rapamycin-insensitive companion of mTOR (Rictor) and stress-activated MAP kinase-interacting protein 1 (Sin1) in mechanistic target of rapamycin complex 2 (mTORC2) [15].

mTORC1 is activated by growth factors and nutrients through Akt-mediated phosphorylation of TSC2. In turn mTORC1 phosphorylates its downstream targets the p70 ribosomal S6 kinase (S6K1) and the eukaryotic initiation factor 4E binding

protein 1 (4E-BP1) and thus stimulates protein synthesis [16].
Autophagy, a catabolic eukaryotic cell process to degrade and digest cell internal proteins or larger structures, is also regulated by mTORC1. If the cell is in an energetically favorable state mTORC1 phosphorylates autophagy related gene 13 (ATG13) and so denies the formation of the autophagy complex[5]. Also anabolic processes like lipid synthesis are coordinated by mTORC1 in consequence of the incitement of the transcription factors sterol regulatory element binding protein 1 (SREBP1) and peroxisome proliferator-activated receptor-γ(PPARγ). Furthermore, mTORC1 has an impact on mitochondrial metabolism and biogenesis through stimulation of PPARγ coactivator 1 (PGC1-α) and yin-yang 1 (YY1). In innate immune cells glycolysis is also promoted by TLR-mediated stimulation of mTORC1.

While the activation mechanism of mTORC1 by growth factors and nutrients

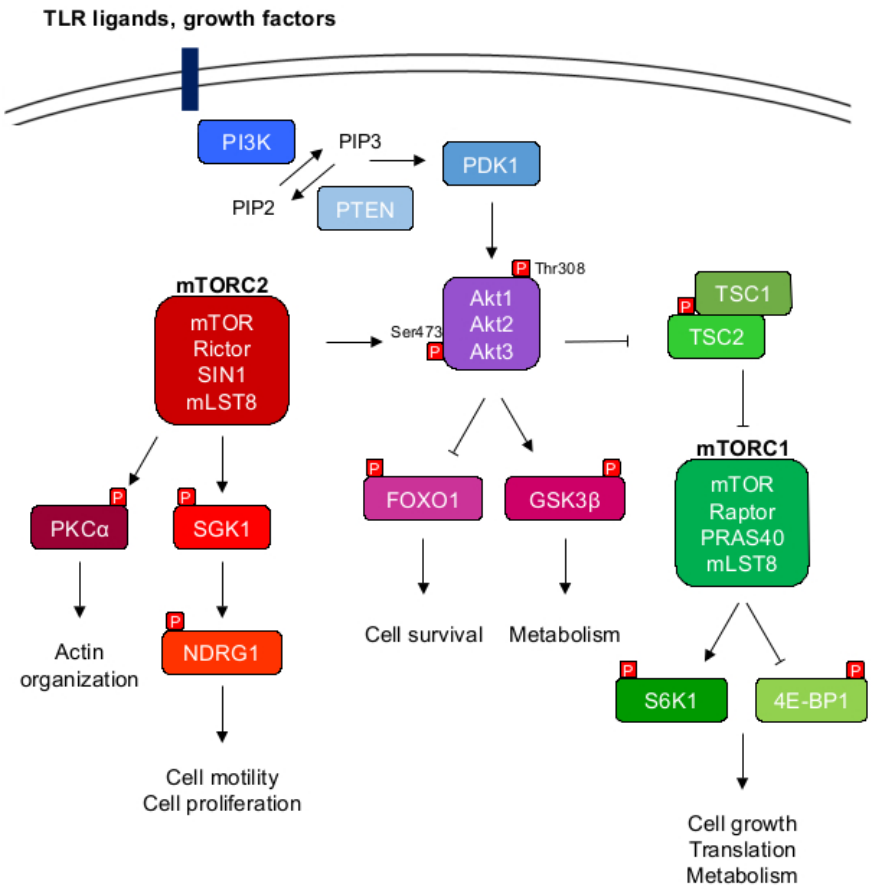

Figure 1.1: Overview of mTORC1 and mTORC2 activation and downstream targets
Figure adpated from Thomas Weichhart, et al [17]

and its function as a pivotal controller of cell growth and metabolism is very well described, the elucidation of the molecular mechanism for activation and regulatory signaling of mTORC2 is still missing. Several localization sites, some depending on the cell cycle state, of mTORC2 have been reported including the

plasma membrane, the nucleus, mitochondria, endoplasmatic reticulum (ER) and the mitochondria associated ER membrane (MAM) [18–21]. Recent studies have shown that upon growth factor or TLR stimulation, the following interaction of phosphatidylinositol (3,4,5)-trisphosphate (PIP3) with the pleckstrin homology like domain (PH) of Sin1 results in the recruitment of the full mTORC2 complex to the plasma membrane to phosphorylate its downstream targets [22].
mTORC2 takes a crucial role in cell survival, metabolism and proliferation due to its prominent downstream target protein kinase B (PKB/Akt). Full Akt activation requires the phosphorylation of its Thr308 site by phosphoinositide-dependent kinase 1 (PDK1) and Ser473 by mTORC2. Knock out of Sin1 or Rictor specifically inhibits phosphorylation of Akt at Ser473, blocks the subsequent phosphorylation of a few Akt substrates, but does not completely abrogate its function. In contrast inhibition of mTORC2 utterly abolishes the activity of serum- and glucocorticoid-induced protein kinase 1 (SGK1), that along with Akt phosphorylates, and thus inactivates, the transcription factors forkhead box protein O1 (FoxO1) and FoxO3a [23]. Cytoskeletal organization is controlled by mTORC2 through promotion of protein kinase Cα (PKCα) phosphorylation, although the molecular regulatory mechanism by which this is achieved remains elusive [24]. Due to its involvement in cytoskeletal organization mTORC2 has also been heavily implicated to affect neutrophil chemotaxis through coordination of myosin II phosphorylation and F-actin polatization [25, 26]. It has been reported that mTORC2 promotes glycolysis metabolism in cancer cells through activation of MYC translation by inactivating class IIa histone deacetylases via phosphorylation, after which follows an inhibiting acetylation of FOXO1 and FOXO3 [27]. Interestingly in these glioblastoma cells an autoactivation loop of mTORC2 is achieved by acetyl-CoA-dependent acetylation of Rictor and maintenance of this acetylation due to elevated glucose levels [28].

1.3 Mouse model

Previous studies have shown that the disrupted expression of Rictor leads to embryonic lethality in mice [29]. Therefore the Cre recombinase-loxP system was used in conjunction with gene targeting techniques to overcome this limitation. Through gene targeting techniques a gene of interest is flanked by two loxP sites, which are 34 bp long nucleotide sequences. These loxP sites are in turn recognized by the cre recombinase and the floxed gene in between is excised [30].

As a vital part of mTORC2 Rictor was selected to be flanked by the loxP sites. De-

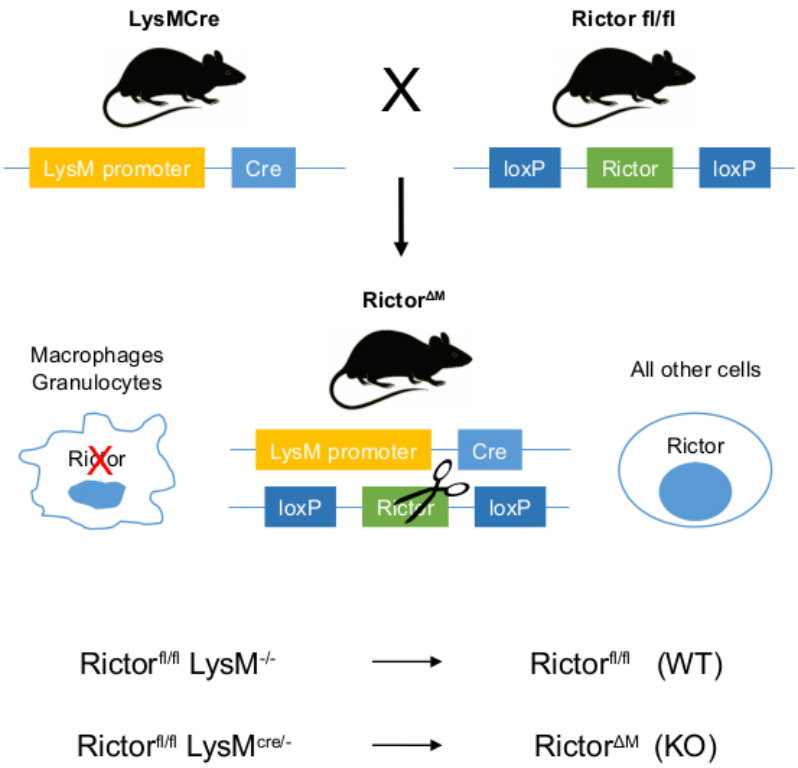

Figure 1.2: Conditional deletion of Rictor strategy and breeding plan.
Figure adapted from Thomas Weichhart

spite the resulting mice containing the floxed Rictor allele in all tissues, they are still phenotypically wildtype and thus used for control macrophages. For a conditional genetic deletion in the myeloid cell lineage the lysozyme M locus was selected for targeted insertion of cre cDNA due to its exclusive expression in myeloid cells upon cell differentiation [31]. To achieve a myeloid specific deletion of Rictor and thus inactivation of mTORC2, the cre expressing mice were bred with their floxed counterparts and thus resulting in a disruption of mTORC2 activity in mature macrophages and granulocytes [32].

2. Aim of the study

As part of the PI3K/Akt signaling axis mTORC2 is activated by growth factors and PAMP stimulation of TLRs [33]. mTORC2 was recently found to be a negative regulator of TLR signaling in macrophages. Recent studies have shown that loss of Rictor, a key component of mTORC2, leads to a hyperinflammatory phenotype in macrophages if challenged with TLR ligands and to high expression levels of M1 marker genes and diminished expression of M2 marker genes [34, 35]. The molecular mechanism of mTORC1 activation and downstream signaling is quite well understood, but still remains elusive for mTORC2 [36].

We were interested in the characterization of the dysfunctional mTORC2 phenotype in mouse macrophages and the impact on macrophage metabolism. Finally we wanted to elucidate the impact of mTORC2 on the molecular mechanism which leads to the hyperinflammatory M1 phenotype in mouse macrophages if Rictor is deleted.

3. Materials and methods

3.1 Buffers, media, solutions

Differentiation media

- Dulbecco's Modified Eagle Medium
- 2 mM L-glutamine
- 100 µg/mL streptomycin
- 100 U/mL penicillin
- 20% L929 culture supernatant
- 10% FCS low endotoxin
- 500 µL mercaptoethanol

DMEM + 10% FCS + Glutamine + Pen/Strep

- Dulbecco's Modified Eagle Medium
- 2 mM L-glutamine
- 100 µg/mL streptomycin
- 100 U/mL penicillin
- 10% FCS low endotoxin
- 500 µL mercaptoethanol

DMEM without Ca^{2+}

- DMEM, high glucose, no glutamine, no calcium
- 0,11 g/L Sodium pyruvate
- 2 mM L-glutamine
- 100 µg/mL streptomycin
- 100 U/mL penicillin
- 500 µL mercaptoethanol

1x PBS

- 1x PBS without Ca^{2+} and Mg^{2+} or phenol red

FACS buffer

- 1x PBS
- 2% FCS low endotoxin
- 1 mM EDTA

Binding buffer

- 0,1 M HEPES
- 1,4 M NaCl
- 25 mM $CaCl_2$

PI solution

- 50 µg/mL Propidium iodide

10x TBS

- 24 g Tris base
- 88 g NaCl
- Dissolve in 800mL distilled water
- Adjust pH to 7.6 with concentrated HCl
- Add distilled water to a final volume of 1L

1x TBS-T

- 200 mL of 10x TBS
- 1798 mL distilled water
- 2 mL Tween 20

10x Protease inhibitor

- 1 Protease inhibitor cocktail tablet
- 2 mL dH_2O

10x Phosphatase inhibitor

- 100 mM NaF
- 20 mM $Na_4P_2O_7$
- 20 mM Glycerophosphat
- 2 mM Na_3VO_4

2x HEPES buffer

- 20 mM Hepes
- 140 mM NaCl
- 2 mM EDTA
- pH 7.9

Lysis buffer

- 50% 2xHEPES
- 10% 10x Protease inhibitor
- 10% 10x Phosphatase inhibitor
- 10% Tx-100
- 20% dH_2O

10x Red blood lysis buffer

- 90 g/L NH_4Cl
- 10 g/L $KHCO_3$
- 0,37 g/L EDTA-Na_2
- Dissolve in 800mL distilled water
- Adjust pH to 7.3
- Add distilled water to a final volume of 1L
- Sterilize by filtration

1x Red blood lysis buffer

- 100 mL 10x Red blood lysis buffer
- 900 mL sterile H_2O

4x Sample buffer

- 250 mM Tris-HCl pH 6.8
- 40% Glycerol
- 8% SDS
- 400 mM Dithiothreitol
- Bromphenolblue

Harlow buffer

- 28,8 g Glycine
- 6,04 g Tris base
- 200 mL Methanol
- 1,6 L dH_2O

10x Running buffer

- 30,28 g/L Tris
- 144,14 g/L Glycine
- 10 g/L SDS
- Dissolve in dH_2O to a final volume of 1L

1x Running buffer

- 100 mL 10x Running buffer
- 900 mL dH_2O

Stacking gel (10mL)	Resolution gel 12% (10mL)	
1,33 mL	4,00 mL	30% AA/Bis (Biorad)
2,50 mL	-	0.5 M Tris-HCl, pH 6.8
-	2,50 mL	1.5 M Tris-HCl, pH 8.8
0,10 mL	0,10 mL	10% SDS
6,07 mL	3,40 mL	dH_2O
10 µL	10 µL	TEMED (Biorad)
100 µL	100 µL	10% APS (Amersham)

Table 3.1: Compounds of stacking and resolution gels used in SDS-PAGE

3.2 Methods

3.2.1 Western Blot

Cells were seeded in 6- or 12- well culture plates, after different conditions of various stimuli the cells were washed with 1xPBS and lysed in 100µL lysis buffer. The lysed cells were sonicated three times for 10 sec and stored on ice for 30 min. Protein concentration was measured via photometry using Bradford solution and an eppendorf BioPhotometer 6131. Sample concentration was adjusted to the same level with lysis buffer and 4x sample buffer was added. Prior to gel loading the samples were

boiled at 95°C for 5 min, then the samples were resolved on a 12% SDS-PAGE and afterwards transferred to a nitrocellulose membrane.
The membranes were blocked for 1h in 1xTBS-T and 4% dry milk, following an incubation with the primary antibody at 4°C over night. After washing the membranes in 1x-TBS-T, an incubation at room temperature for 45 min with the corresponding secondary antibodies in 4% dry milk was conducted. Chemiluminescence was used for protein detection with the application of Pierce™ ECL Western Blotting Substrate (Thermo Fisher) on the membranes and visualized through Amersham Hyperfilm ECL (GE-Healthcare) and an Medical X-ray Processor 2000 (Kodak).

Primary antibodies	Dilution	Origin	Company
Rictor	1:1000	rabbit	Cell signaling
p-Akt^{Ser473}	1:1000	rabbit	Cell signaling
p-Akt^{Thr308}	1:1000	rabbit	Cell signaling
pan Akt	1:2000	mouse	Cell signaling
p-NDRG1^{Thr346}	1:1000	rabbit	Cell signaling
p-p70S6K^{Thr389}	1:1000	rabbit	Cell signaling
p-S6 (240/244)	1:2000	rabbit	Cell signaling
p-Rb	1:1000	rabbit	Cell signaling
p27(Kip1)	1:1000	rabbit	Santa Cruz Biotechnology
4E BP1	1:1000	rabbit	Cell signaling
p44/42 MAPK (Erk1/2)	1:1000	rabbit	Cell signaling
GRP78	1:1000	rabbit	Santa Cruz Biotechnology
GADD153/CHOP	1:1000	rabbit	Santa Cruz Biotechnology
GAPDH	1:1000	rabbit	Cell signaling
Histon H3	1:1000	rabbit	Cell signaling
Secondary antibodies	Dilution	Origin	Company
Anti-rabbit	1:10000	donkey	Bethyl Laboratories
Anti-mouse	1:10000	goat	Bethyl Laboratories

Table 3.2: Antibodies used for Western Blot
Primary antibodies were diluted in PBS-T + 0,02% NaN_3
Secondary antibodies were diluted in 1xTBS-T + 4% dry milk

3.2.2 Bone marrow extraction

After the mouse is euthanized, both hind limbs are carefully removed. Femur and Tibia of both legs are cleaned, briefly sterilized in 70% EtOH and stored in DMEM for further use. Under sterile conditions both ends of the femur and tibia are removed and the bone marrow is flushed out by injecting 15mL differentiation media (or DMEM if the bone marrow is intended for long term storage in liquid nitrogen) with a 27g needle into the bone. The flushed bone marrow cell suspension is centrifuged at 350 rcf for 5 min at 4°C and resuspended in 1xPBS. If the bone marrow is to be

seeded immediately, then $\frac{1}{5}$ of the resuspended cell suspension is again centrifuged at 350 rcf for 5 min at 4°C and then resuspended in 12mL differentiation medium and seeded on a 10cm petri dish.
The remaining $\frac{4}{5}$ are also centrifuged at 350 rcf for 5 min at 4°C, resuspended in 3mL 1x red blood lysis buffer and incubated for 3 min. Afterwards the reaction is stopped by adding 7mL 1xPBS + 2% FCS and another centrifugation step. Again the pellet is resuspended in 10mL 1xPBS + 2% FCS and after another centrifugation step, the pellet is resuspended in 1800µL. In the end 900µL bone marrow cell suspension is transferred into a cryotube, mixed with 100µL DMSO, stored on ice for 20 min, afterwards the cryotubes are transferred into a Mr.Frosty™ Freezing Container and put on -80°C overnight. Finally on the next day the cryotubes are stored in liquid nitrogen.

3.2.3 Peritoneal macrophage extraction

The mouse is anesthetized via Ketasol injection and euthanized (then the spinal cord is broken by applying physical force). Afterwards the cadaver is sterilized by spraying it with 70% EtOH and the skin is carefully removed without harming the abdominal wall. Without puncturing any organs 10mL of ice cold 1xPBS are injected with a 27g needle into the peritoneal cavity following a gentle massage of the cavity to dislodge attached cells. A 20g needle attached to a 10mL syringe is inserted into the peritoneum and as much cell suspension as possible is extracted and stored on ice. The cell suspension is centrifuged at 350 rcf at 4°C for 7 min, the supernatant is discarded and the pellet is resuspended in 3mL red blood lysis buffer. After 3 min the reaction is stopped by adding 7mL 1xPBS + 2% FCS and another centrifugation step at 350 rcf and 4°C for 7 min. Again the supernatant is discarded and the pellet is resuspended in 10mL 1xPBS + 2% FCS. In the end the cells are counted and seeded or used for experiments.

3.2.4 Generation of bone marrow-derived macrophages

A cryotube containing $\frac{1}{5}$ of the extracted bone marrow is thawed at 37°C in a water bath and seeded on a 10cm non cell culture treated dish in 12mL differentiation media. At the 3rd day the cells are washed with 37°C 1xPBS and 12mL of fresh differentiation media are added. The cells are scraped and split 1:2 on the 4th day on new non cell culture treated 10cm dishes and finally on the 6th day the cells are to be scraped, counted and seeded for experiments.

3.2.5 Scratch assay

The scratch areas were marked beforehand on a 24 well plate and the macrophages were seeded under 3 different media conditions:

- DMEM + 10% FCS
- DMEM + 10% FCS + 20% L929 culture supernatant
- DMEM + 10% FCS + LPS [1000 µg/mL]

Using a 1mL pipette tip a linear scratch was made and pictures were taken with a light microscope at various time points. The pictures were analyzed with Fiji [37].

3.2.6 Annexin V - PI Apoptosis assay

After harvesting the cells by pipetting, they were centrifuged at 350 rcf at 4°C for 5 min, the supernatant was discarded and the macrophages were resuspended in 200µL binding buffer. Following which the cells were incubated with 5µL Annexin V antibody for 20min on ice and 1µL PI (1mg/mL) was added to the sample right before the flow cytometric measurement with a FACSCalibur (BD Bioscience). Resulting data were analyzed with FlowJo (Tree Star Inc, Ashland, OR).

3.2.7 Cell cycle analysis

Macrophages were starved in DMEM containing 0% FCS for 24h and reactivated with M-CSF (100ng/mL). At different time points the cells were scraped on ice and centrifuged at 350 rcf and 4°C for 5 min. The supernatant was discarded and cells were resuspended in 150µL 1xPBS. While the samples were gently vortexed, 750µL ice cold 85% ethanol was added and then stored at -20°C. Samples obtained this way can be stored up to 6 months. After a minimum of 24h the samples were centrifuged at 1000 rpm and 4°C for 10 min and the supernatant discarded. Following which the cells were resuspended in 300µL PI-solution (50µg/mL) and incubated in the absence on light and on ice for 20 min. Another centrifugation at 1000 rpm at 4°C for 10 min follows, afterwards the supernatant is discarded and the cells resuspended in 200µL FACS buffer and ready for measurement with a FACSCalibur (BD Bioscience). Resulting data were analyzed with FlowJo (Tree Star Inc, Ashland, OR).

3.2.8 Cell cycle analysis with peritoneal macrophages

Peritoneal macrophages are obtained as described in 3.2.3. The cells are centrifuged at 350 rcf at 4°C for 7 min, afterwards the supernatant is discarded and the pellet

is resuspended in 50µL FACS buffer. A 10µL mixture of 9µL FACS buffer and 1µL TruStain fcX™ (anti-mouse CD16/32) antibody is added to each sample and the samples are incubated in the dark and on ice for 5 min. Next CD115 FITC is added as a surface marker for peritoneal macrophages, as a mixture of 10µL FACS buffer containing 0.25µL antibody, to the cells and a final incubation in the dark and on ice for 20 min is conducted. In the end the samples are centrifuged at 350 rcf at 4°C for 7 min, the supernatant is discarded and the pellet resuspended in 150µL 1xPBS. Afterwards the protocol described at 3.2.7 is continued.

3.2.9 2-NBDG uptake

The cells are resuspended from the X-well plate by gently pipetting up and down. After centrifugation at 350 rcf for 5 min, the supernatant is discarded and the pellet is resuspended in 50µL 37°C 1xPBS. Furthermore 50µL 37°C 2-NBDG (c=200µM) are added to a final concentration of 100µM 2-NBDG in each sample and the samples are incubated in the absence of light at 37°C for 10 min. Afterwards the samples are immediately put on ice and 2 washing steps follow, where 1mL ice cold 1xPBS is added to each sample and furthermore the samples are centrifuged at 350 rcf at 4°C for 5 min. In the end the supernatant is discarded and the samples resuspended in 250µL FACS buffer to be analyzed by a FACSCalibur (BD Bioscience). Resulting data were analyzed with FlowJo (Tree Star Inc, Ashland, OR).

3.2.10 2-NBDG uptake with peritoneal macrophages

As described in 3.2.8, but F4/80 APC is used as a surface marker for peritoneal macrophages (0.5µL antibody for each sample) instead of CD115 FITC. In the end the pellet is resuspended in 50µL 37°C 1xPBS and the protocol described at 3.2.9 is continued.

3.2.11 Mitotracker Green FM

The cells are resuspended from the X-well plate by gently pipetting up and down. After centrifugation at 350 rcf for 5 min, the supernatant is discarded and the pellet is resuspended in 50µL 37°C 1xPBS. Furthermore 50µL 37°C Mitotracker Green FM (c=120nM) are added to a final concentration of 60nM Mitotracker Green FM in each sample and the samples are incubated in the absence of light at 37°C for 30 min. Afterwards the samples are immediately put on ice, washed with 1mL ice cold 1xPBS and furthermore the samples are centrifuged at 350 rcf at 4°C for 5 min. In the end the supernatant is discarded and the samples resuspended in 200µL FACS

buffer, to be analyzed by a FACSCalibur (BD Bioscience). Resulting data were analyzed with FlowJo (Tree Star Inc, Ashland, OR).

3.2.12 Mitotracker Red CMX Ros

Same procedure as described in 3.2.11, but Mitotracker Red CMX Ros, with a final concentration of 30nM per sample, is used instead of Mitotracker Green FM.

3.2.13 Antibodies and dyes used in flow cytometry

Antibodies	Conjugate	Clone	Company
Annexin V	Alexa Fluor 488		Life Technologies
CD115	Alexa Fluor 488	AFS98	ebioscience
F4/80	APC	BM8	Biolegend
Dyes	Concentration		Company
Mitotracker Green FM	60nM		Thermo Fisher Scientific
Mitotracker Red CMX Ros	30nM		Thermo Fisher Scientific
2-NBDG	100µM		Thermo Fisher Scientific

Table 3.3: Antibodies and dyes used in flow cytometry

4. Results

4.1 Deletion of Rictor abrogates Akt phosphorylation at Ser473

For validation of the successful conditional genetic deletion of Rictor an immunoblot analysis was done with bone marrow-derived macrophages (BMDM) and peritoneal macrophages. Rictor was successfully deleted in both bone marrow-derived and peritoneal Rictor$^{\Delta M}$ macrophage lines (Figure 4.1). Although there was no difference in p-Akt^{Thr308} abundance, p-Akt^{Ser473} was decreased in the Rictor$^{\Delta M}$ macrophages. In line with these results we found less p-NDRG1, also downstream target of mTORC2, in Rictor$^{\Delta M}$ and no differences in p-p70S6K and 4E BP1, both mTORC1 downstream targets, protein levels.

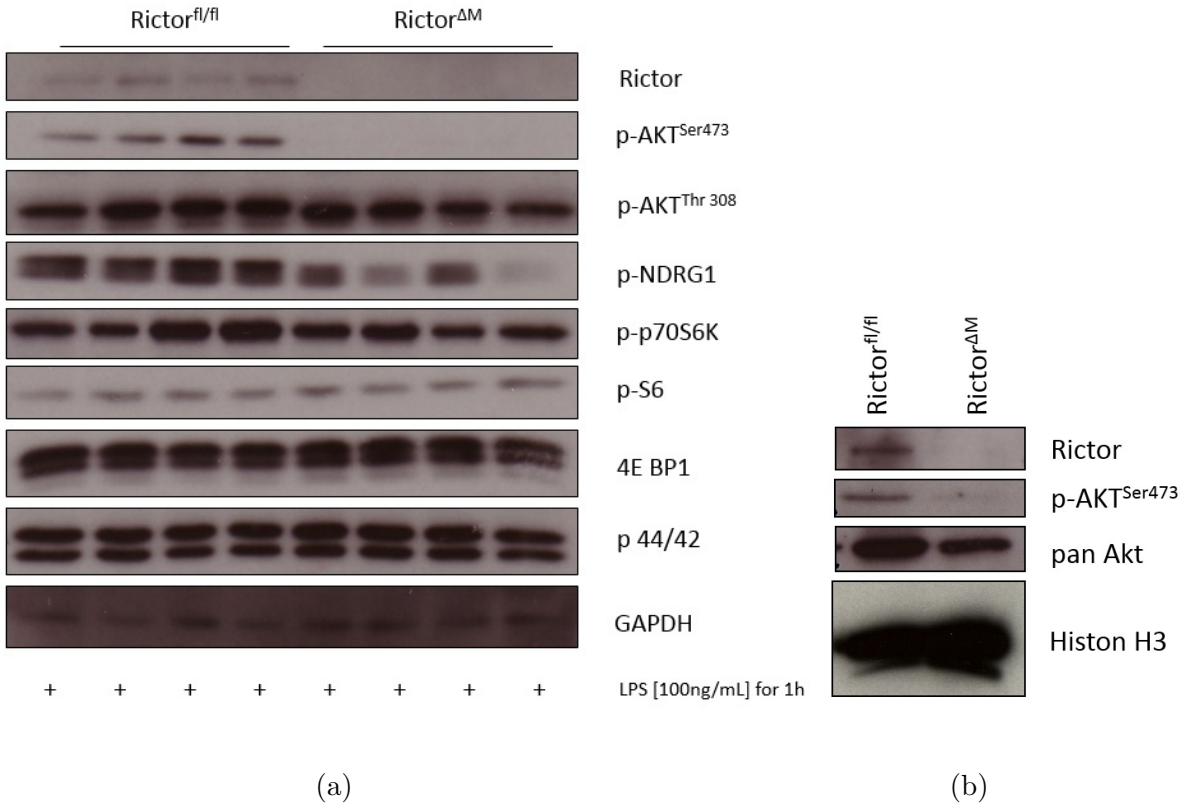

Figure 4.1:
(a) Immunoblot analysis of BMDM that have been stimulated with LPS (100ng/mL) for 1h
(b) Immunoblot analysis of mouse peritoneal macrophages

4.2 No significant difference in wound healing

Tissue homeostasis and wound healing are important tasks that are performed by M2-polarized macrophages and to test if the wound healing and migration ability of Rictor$^{\Delta M}$ macrophages is impaired, we performed a scratch assay. Rictor$^{\Delta M}$ and control (Rictor$^{fl/fl}$) macrophages were seeded in a 24 well plate and pictures were taken at two time points. As expected the scratch area diminished the most in media containing either M-CSF or LPS stimulated macrophages (Figure 4.2). Interestingly we did not observe significant differences in the receding scratch area between control and Rictor$^{\Delta M}$ macrophages.

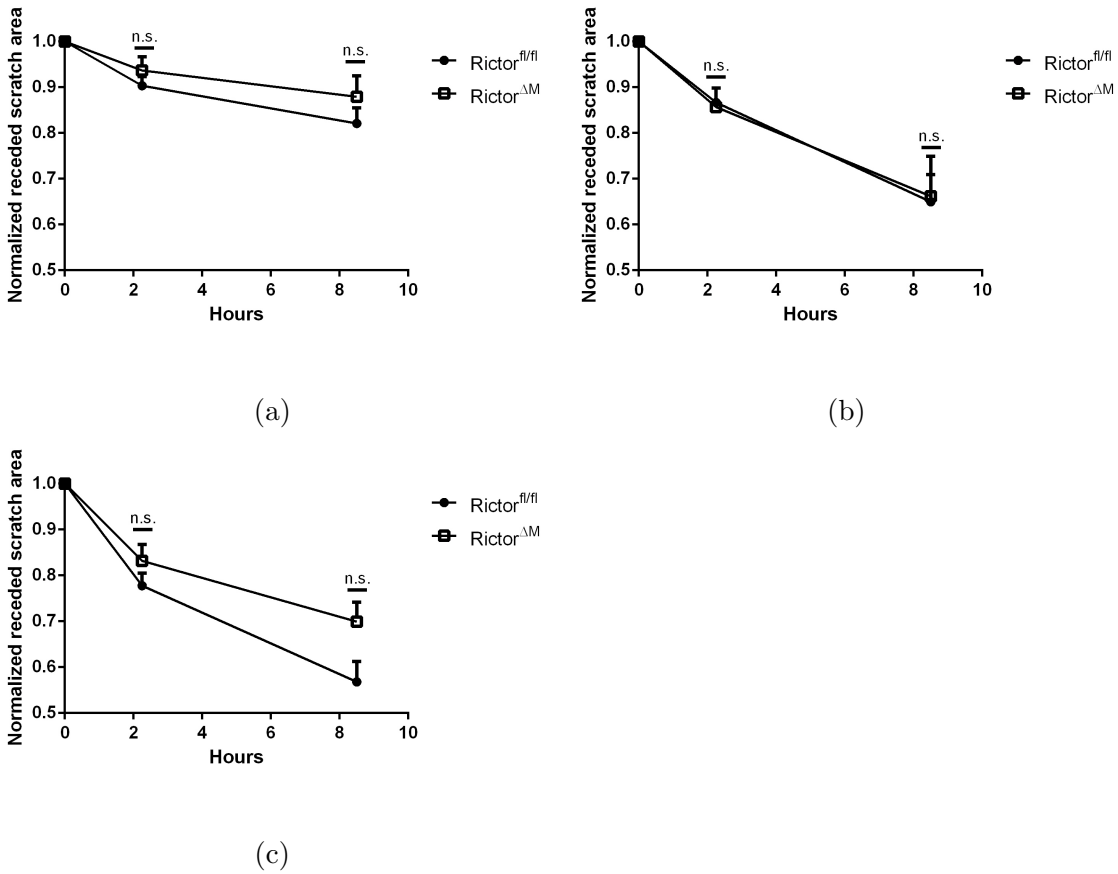

Figure 4.2: Scratch assay with time points taken 2h15min and 8h30min after restimulation
(a) DMEM with 10% FCS
(b) DMEM stimulated with LPS (100ng/mL)
(c) DMEM with 20% L929 culture supernatant
Data is shown as means of normalized receded scratch area + SEM with an initial scratch area of 9×10^6 pixel^2, n$\geq$5

4.3 Increased apoptosis of Rictor$^{\Delta M}$ macrophages during prolonged nutrient deprivation

As mTORC2 has a crucial role in cell survival and metabolism we wanted to investigate its impact in macrophages. In order to accomplish that, Rictor$^{\Delta M}$ and Rictor$^{fl/fl}$ macrophages were seeded in 6 well plates and in medium with 10% FCS or without FCS. After the cells were confluent 20% L929 culture supernatant, 0.5µM staurosporine (STS), a protein kinase inhibitor, or 1µM STS was added to the wells containing medium with 10% FCS. Following an incubation time of 2h the first samples were taken and 48h later a second set of samples were acquired and analyzed via flow cytometry (Figure 4.3).

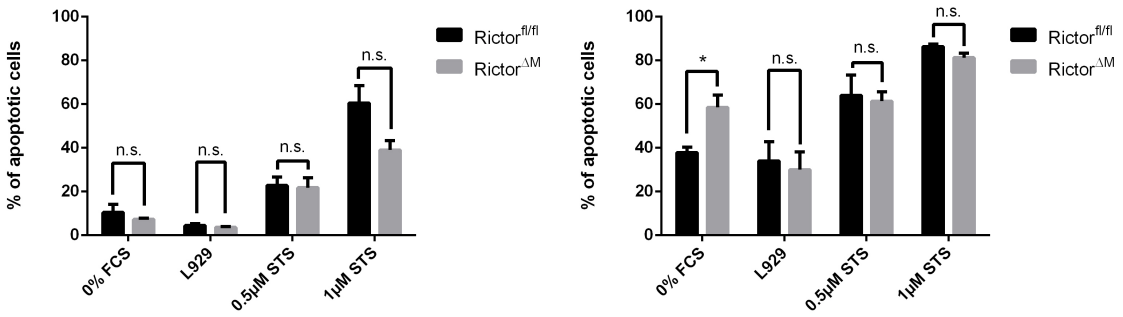

(a) (b)

Figure 4.3:
(a) Samples taken after 2h of nutrient starvation, growth factor stimulation or staurosporine (0.5µM, 1µM) stimulation
(b) Samples taken after 48h of nutrient starvation, growth factor stimulation or staurosporine (0.5µM, 1µM) stimulation
Flow cytometric assessment of apoptotic cells via Annexin V - PI staining was performed. Data is shown as means + SEM of the percentage of Annexin V and PI positive cells, n=3, Statistical analysis was done by a two sample t test, $* \; p \leq 0.05$

In line with our expectations the STS treated samples showed a higher abundance of apoptotic cells at either time point compared to nutrient starved or growth factor treated cells.
Surprisingly contrary to previous studies and our expectations there were no significant differences in the amount of apoptotic cells in either media 2 hours post treatment. As expected, compared to control macrophages, loss of mTORC2 function led to a significantly higher apoptosis rate in Rictor$^{\Delta M}$ macrophages that were nutrient deprived for a period of 48h.

4.4 Loss of Rictor leads to cell cycle lag in macrophages

Next we looked into cell cycle progression, because mTORC2 downstream targets SGK1 and Akt phosphorylate and thus inactivate transcription factors FoxO1 and FoxO3a, which are implicated in the expression of various genes involved in cell cycle arrest [23].

In order to analyze cell cycle advancement in macrophages, we seeded Rictor$^{\Delta M}$ and control, bone marrow-derived and peritoneal, macrophages in 6 well plates and serum starved them for 24h to arrest the cells in G1 phase. Afterwards we changed the medium and added M-CSF(100ng/mL) to simultaneously initiate cell cycle progression in all cells. The cells were harvested at indicated time points and subjected to flow cytometric analysis.

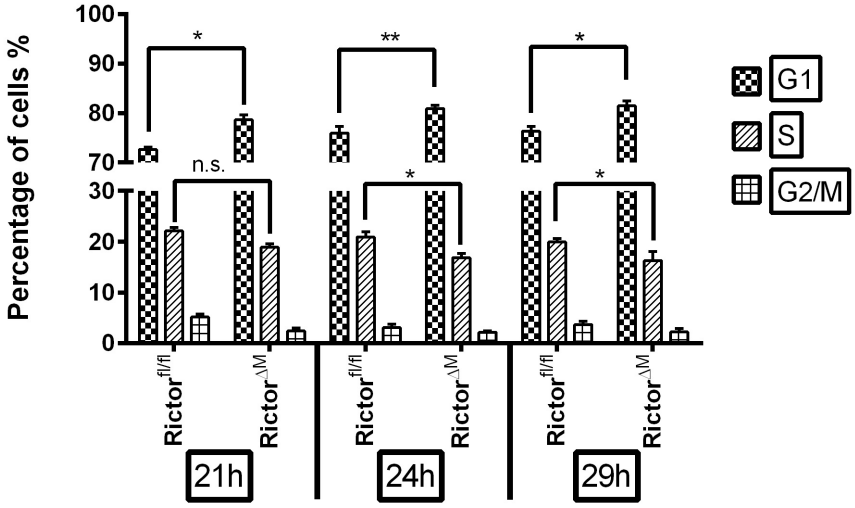

Figure 4.4: Flow cytometric analysis of cell cycle with propidium iodide DNA staining in Rictor$^{fl/fl}$ and Rictor$^{\Delta M}$ bone marrow-derived macrophages after a 24h starvation period following restimulation with M-CSF(100ng/mL). Samples were taken at the indicated time points after M-CSF restimulation. Data is shown as means + SEM, n=4, Statistical analysis was done by a two sample t test, $*$ $p \leq 0.05$, $**$ $p \leq 0.01$

A significant cell cycle lag from G1 to S phase in Rictor$^{\Delta M}$ macrophages was observed 24h after restimulation with M-CSF, both in vitro (Figure 4.4) and ex vivo (Figure 4.5).

To investigate the molecular mechanism a western blot analysis after a 24h incubation period in 0%, 2% and 10% FCS was conducted.

Rictor$^{\Delta M}$ macrophages showed less abundance of p-Rb (Figure 4.6). Akt-mediated phosphorylation of Rb is important for cell cycle progression from G1 to S phase

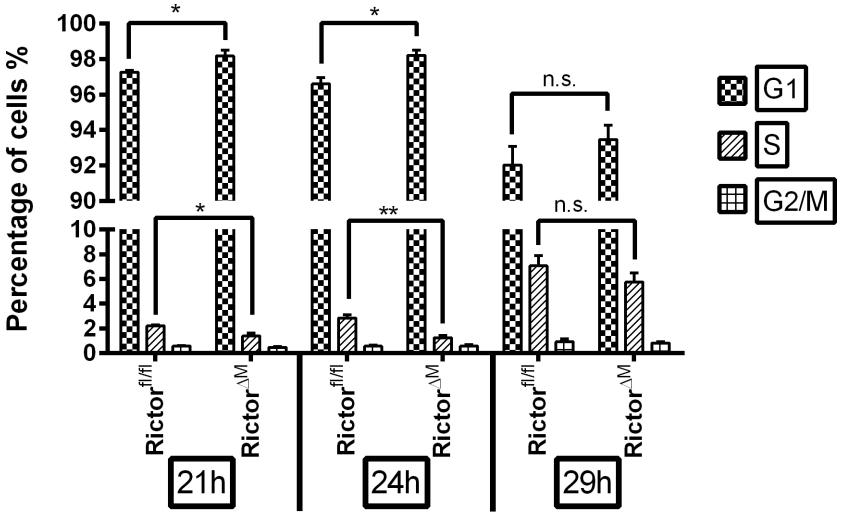

Figure 4.5: Flow cytometric analysis of cell cycle with propidium iodide DNA staining in Rictor$^{fl/fl}$ and Rictor$^{\Delta M}$ peritoneal macrophages after a 24h starvation period following restimulation with M-CSF(100ng/mL). Samples were taken at the indicated timepoints after M-CSF restimulation. Data is shown as means + SEM, n=3, Statistical analysis was done by a two sample t test, $*$ $p \leq 0.05$, $**$ $p \leq 0.01$

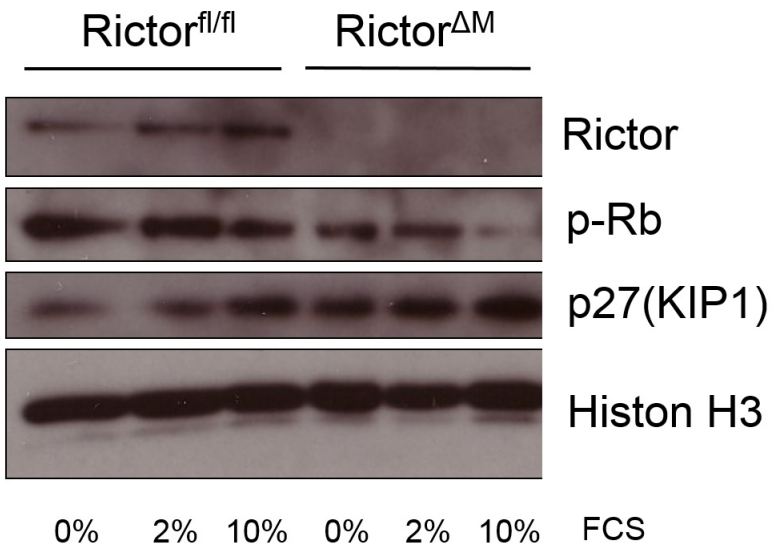

Figure 4.6: Western blot analysis of Rictor$^{fl/fl}$ and Rictor$^{\Delta M}$ bone marrow-derived macrophages after after a 24h incubation period in 0%, 2% and 10% FCS

[38]. Interestingly higher amounts of p27(KIP1), a cell cycle inhibitor and direct downstream target of p-Akt [39], were also found in Rictor$^{\Delta M}$ macrophages.
The data suggests that the lag in G1 to S phase progression in bone marrow-derived and peritoneal Rictor$^{\Delta M}$ macrophages may be attributed to a higher abundance of p27(KIP1) and low levels of p-Rb.

4.5 mTORC2 controls glucose uptake

In our lab group it was recently shown that deletion of Rictor in macrophages leads to significantly higher expression of M1 markers when stimulated with LPS/IFNγ (Figure 4.7 c) and significantly lower amounts of M2 markers when stimulated with IL-4, than observed in control macrophages (Figure 4.7 a,b).

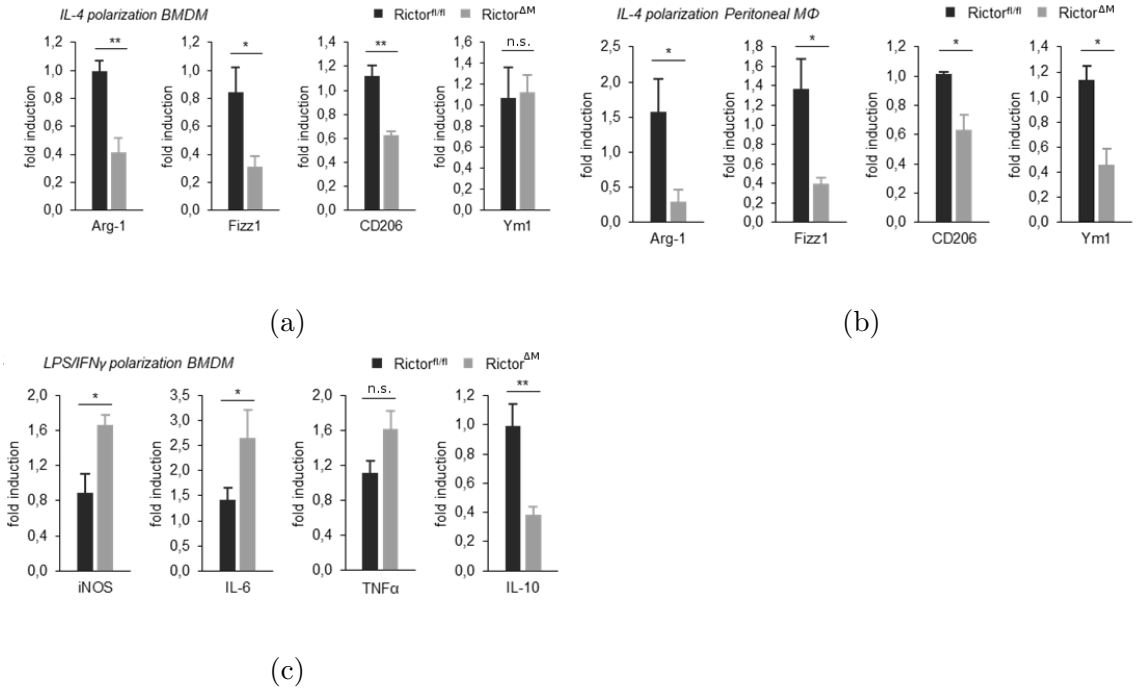

Figure 4.7: mRNA levels of M1 and M2 marker proteins in BMDM and peritoneal macrophages stimulated for 48h with either LPS (100ng/mL) and IFNγ (20ng/mL) (c) or IL-4 (10ng/mL) (a, b) were measured by q-PCR and normalized to β-actin, Data is shown as fold induction + SEM, Statistical analysis was done by a two sample t test, $*$ $p \leq 0.05$, $**$ $p \leq 0.01$, $n \geq 4$
Figures adapted from Katholnig, Schuetz et al

Depending on environmental stimuli macrophages can either polarize to a proinflammatory M1, a tissue homeostasis M2 phenotype, or any spectrum in between and that M1-polarized macrophages rely on a glycolytic metabolism [10, 11, 14].
In order to test the impact of mTORC2 on the glucose uptake Rictor$^{\Delta M}$ and control macrophages were treated with either LPS or IL-4 and the 2-NBDG uptake, a fluorescent glucose analog, was measured by flow cytometry. The same analysis was also done with unstimulated peritoneal macrophages.

In line with previous studies [40] unstimulated ex vivo Rictor$^{\Delta M}$ peritoneal macrophages (Figure 4.8b) and LPS stimulated bone marrow-derived Rictor$^{\Delta M}$ macrophages exhibited a significantly lower 2-NBDG uptake than control

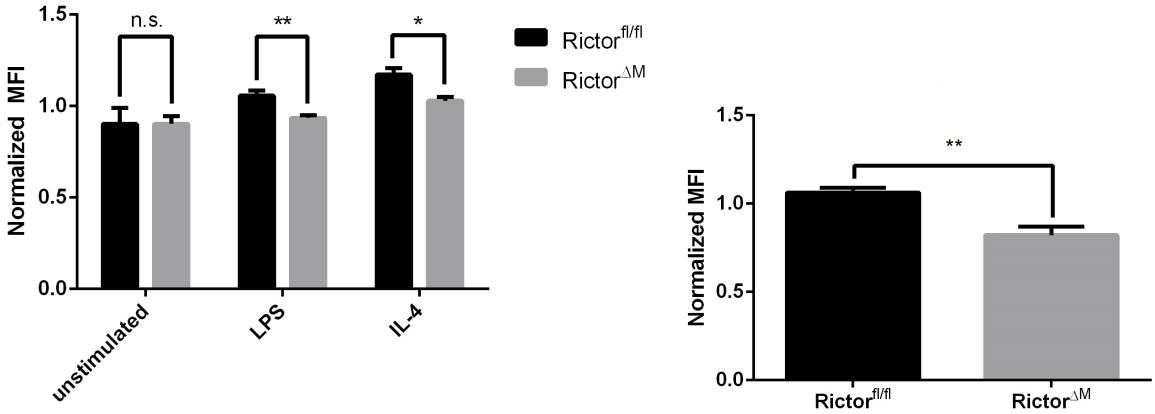

(a) (b)

Figure 4.8: Flow cytometric measurement of 2-NBDG uptake into the cells.
(a) BMDM were either stimulated with LPS (100ng/ml) or IL-4 (20ng/mL) for 24h and 2-NBDG uptake was measured afterwards, n≥3
(b) Obtained peritoneal cells are stained with F4/80 APC for macrophages and 2-NBDG uptake was measured, n≥5
Data is shown as means of fluorescent intensity + SEM, Statistical analysis was done by a two sample t test, $*$ p≤0.05, $**$ p≤0.01

macrophages. Interestingly also IL-4 stimulated Rictor$^{\Delta M}$ macrophages had a significantly lower rate of 2-NBDG uptake (Figure 4.8a).
Following these results and to get further insight if the diminished glucose uptake and therefore reduced glycolytic activity of Rictor$^{\Delta M}$ macrophages may be linked to their deficiency in M2 polarization we stimulated Rictor$^{\Delta M}$ and control macrophages with IL-4 and 2-DG, a glycolytic inhibitor and conducted a quantitative PCR analysis.

After IL-4 stimulation the expression of M2 marker gene Arg-1 in control macrophages was down regulated by 2-DG to a similar extent as observed in untreated Rictor$^{\Delta M}$ macrophages and also 2-DG could not further downregulate Arg-1 expression in Rictor$^{\Delta M}$ macrophages.
These data implicate that mTORC2 plays an important role in the ability to take up glucose in macrophages and that M2 polarization is also dependent on glycolysis.

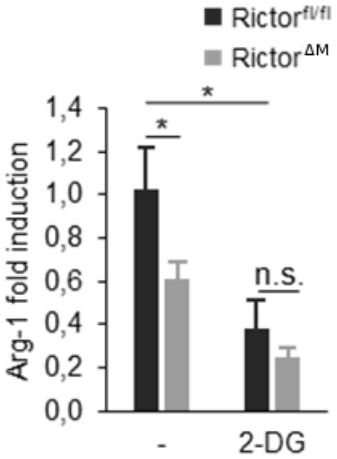

Figure 4.9: mRNA levels of M2 marker protein Arg-1 in BMDM stimulated with IL-4 (20ng/mL) and one set of samples treated with the glycolytic inhibitor 2-DG (5mM), were measured by q-PCR and normalized to β-actin, Data is shown as fold induction + SEM, Statistical analysis was done by a two sample t test, $*$ $p \leq 0.05$, n=4
Figure adapted from Katholnig, et al

4.6 Rictor$^{\Delta M}$ macrophages exhibit diminished mitochondrial membrane potential and elevated ER-stress

It is known that M2-polarized macrophages rely more heavily on mitochondrial respiration for energy production [10] and mTORC2 has been reported to be located at the mitochondria-associated endoplasmic reticulum membranes (MAM) [21]. With recent studies and our previous observations in mind we wanted to test if the attenuated M2 polarization of Rictor$^{\Delta M}$ macrophages can be attributed to a mTORC2-deficiency-mediated disturbed mitochondrial physiology. Therefore we used Mitotracker Green FM to measure mitochondrial mass and Mitotracker Red CMX Ros to ascertain the mitochondrial membrane potential ($\Delta\Psi$) via flow cytometry [41].

We encountered significant lower $\Delta\Psi$ in unstimulated Rictor$^{\Delta M}$ compared to control macrophages, but interestingly no difference in mitochondrial mass (Figure 4.10 a,b).

Recent studies accredited mTORC2 a pivotal role in regulating the Ca^{2+} release from the ER into the cytosol [42]. Surprisingly contrary to our findings it was previously reported that impaired mTORC2 activity leads to an increase in $\Delta\Psi$ due to missing mTORC2/Akt-mediated phosphorylation of HK2 and thus stabilization of the voltage-dependent anion-selective channel 1 (VDAC1) trimeric complex at the MAM [21].

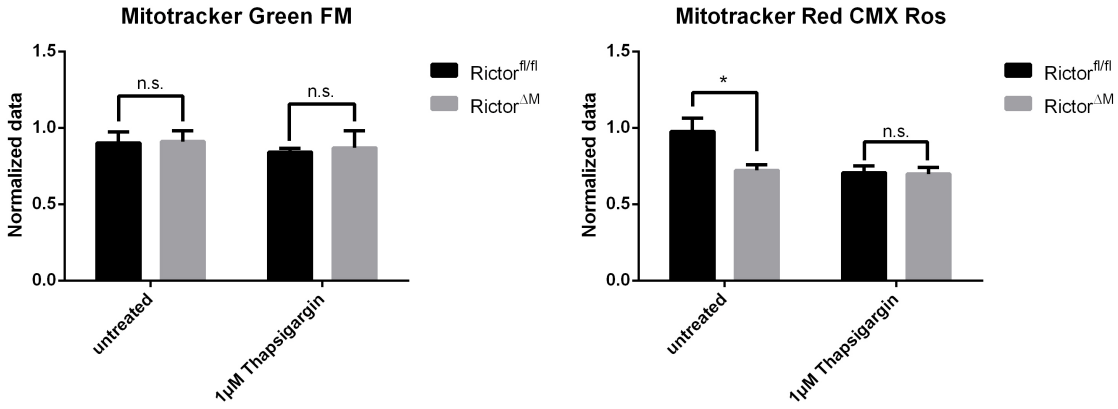

(a) (b)

Figure 4.10:
(a) Flow cytometric measurement of Mitotracker Green FM (60nM) was used to ascertain mitochondrial mass of Rictor$^{fl/fl}$ and Rictor$^{\Delta M}$ macrophages treated with thapsigargin (1µM) for 21h.
(b) Flow cytometric measurement of Mitotracker Red CMX Ros (30nM) was used to ascertain $\Delta\Psi$ of Rictor$^{fl/fl}$ and Rictor$^{\Delta M}$ macrophages treated with thapsigargin (1µM) for 21h.
Data is shown as normalized mean fluorescent intensity + SEM, Statistical analysis was done by a two sample t test, $*$ $p \leq 0.05$, $n \geq 4$

To test if the diminished $\Delta\Psi$ in Rictor$^{\Delta M}$ macrophages can be accredited to a constant Ca^{2+} release into the cytosol due to a dysfunctional inhibition of the inositol 1,4,5-trisphosphate receptor (IP3R), a Ca^{2+} release channel on the ER membrane, by mTORC2 activated Akt, we treated Rictor$^{fl/fl}$ and Rictor$^{\Delta M}$ BMDM with thapsigargin, an IP3 independent intracellular calcium releaser [43, 44].
Interestingly Rictor$^{fl/fl}$ and Rictor$^{\Delta M}$ macrophages showed the same $\Delta\Psi$ levels following a 2h treatment with thapsigargin (Figure 4.10 b), suggesting that the loss of $\Delta\Psi$ in Rictor$^{\Delta M}$ macrophages can be attributed to a dysfunctional intracellular Ca^{2+} flux.

Thapsigargin is also an inducer of ER Stress and previous studies showed increased inflammatory immune response in macrophages due to a disrupted intracellular calcium flow and activation of the unfolded protein response (UPR)[45–48].
In order to investigate an early onset of the UPR in Rictor$^{\Delta M}$ macrophages we performed a western blot analysis (Figure 4.11) and in line with our expectations found elevated GRP78/Bip and GADD25/CHOP protein levels in Rictor$^{\Delta M}$ bone marrow-derived and peritoneal macrophages.
The increased GRP78/Bip and GADD25/CHOP abundance in Rictor$^{\Delta M}$ macrophages provides further evidence that mTORC2 has a positive impact on maintaining ER and mitochondria homeostasis.

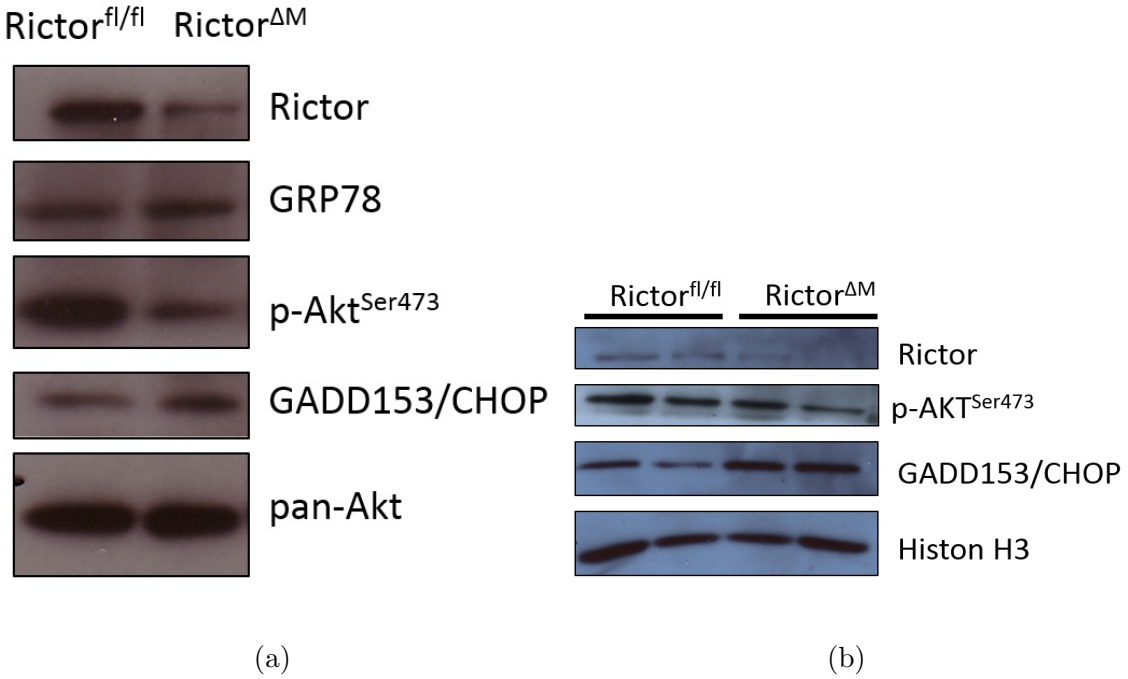

Figure 4.11: Immunoblot analysis of endoplasmatic reticulum stress marker proteins GRP78 and GADD153/CHOP.
(a) Unstimulated bone marrow-derived macrophages
(b) Unstimulated ex vivo peritoneal macrophages

Together these results suggest that mTORC2 plays a key part in mitochondrial metabolism, ER homeostasis and M2 polarization.

5. Discussion

In this study we showed that loss of Rictor in macrophages leads, in vitro and ex vivo, to a distinct lag in G1 to S phase progression probably due to decreased Akt-mediated phosphorylation of Rb [29, 49, 50] and to increased apoptosis after 3 days of serum deprivation [51–53] as has been reported in other cells. Furthermore it has been described that Rictor deletion severely inhibits neutrophil chemotaxis [25], but in our experiments we didn't discern a difference in macrophage mobility and we could also confirm the hyperinflammatory phenotype of Rictor$^{\Delta M}$ macrophages [34, 35].

As Rictor$^{\Delta M}$ macrophages exhibited elevated expression of M1 marker genes, we analyzed the glucose uptake as M1 macrophages heavily rely on glycolysis as their primary energy source [54]. Interestingly we found that mTORC2 disruption leads to a significantly decreased glucose uptake in either LPS or IL-4 stimulated Rictor$^{\Delta M}$ macrophages.

In addition we investigated the difference in $\Delta\Psi$ as indicator for oxidative phosphorylation, which is primarily used by M2-polarized macrophages for energy generation. We found that Rictor$^{\Delta M}$ macrophages had a significantly lower $\Delta\Psi$, which suggests not an increased glucose uptake but impairment of mitochondrial oxidative phosphorylation leads to the increased M1 polatization of Rictor$^{\Delta M}$ macrophages.

Furthermore our q-PCR data implies that glycolysis is important for M2 polarization, because through the use of the glycolytic inhibitor 2-DG we were able to decrease the Arg1 expression of IL-4 stimulated control macrophages to the same level as Rictor$^{\Delta M}$ macrophages.

With our $\Delta\Psi$ data in mind and as mTORC2 has been reported to localize at the MAM, we used the intracellular calcium releaser thapsigargin to reduce $\Delta\Psi$ in Rictor$^{fl/fl}$ to the same amount as in Rictor$^{\Delta M}$ macrophages.

Moreover we discerned increased in vitro and ex vivo levels of ER stress marker proteins GRP78 and GADD135/CHOP in Rictor$^{\Delta M}$ macrophages, which together with our previous data hints at the important role of mTORC2 in alleviating ER stress in macrophages.

First of all we confirmed the efficacy of the macrophage specific deletion of Rictor in vitro and ex vivo. In line with previous studies [55] the conditional deletion of Rictor resulted in less abundant activation of mTORC2 downstream targets p-Akt^{Ser473} and p-NDRG1, while protein levels of mTORC1 downstream target p-p70S6K remained unaffected (Figure 4.1).

Next we looked at macrophage mobility, because it has been reported that Rictor loss leads to impaired chemotaxis in neutrophils and cancer cells [25, 56]. Therefore we applied a scratch assay to assess wound healing ability of Rictor$^{\Delta M}$ macrophages. In line with our expectations cell migration was enhanced in media containing either LPS or M-CSF, but interestingly we couldn't discern any difference in the in vitro wound healing capability (Figure 4.2). We also performed a cell migration assay with a growth factor gradient as chemoattractant, but didn't encounter a difference either (data not shown).
He et al. showed that Rictor dependent loss of chemotaxis in neutrophils happens due to reduced activities of Rac and Cdc42, which are both powerful regulators of neutrophil chemotaxis and actin polymerization, in a mTORC2 independent manner. Further analysis remains as the precise mechanism how mTORC2 regulates actin dynamics is still elusive.

Afterwards we analyzed the cell viability of Rictor$^{\Delta M}$ macrophages as the literature points to an increased rate of apoptosis in case of mTORC2 dysfunction [51–53]. In addition to nutrient depleted and growth factor supplemented media we also added the protein kinase inhibitor staurosporine in two different concentrations to the samples in our assumption that Rictor$^{\Delta M}$ macrophages would loose cell viability faster than control macrophages [57].
We assessed cell viability by flow cytometric measurement of Annexin V - PI staining, which are indicators for early and late stage apoptosis and took samples 24 and 72 hours post stimulation or nutrient deprivation. Surprisingly there was no significant difference in apoptotic cells after 24 hours in either condition (Figure 4.3a). Although in line with our expectations, after 72 hours we found a significant higher amount of apoptotic Rictor$^{\Delta M}$ macrophages under starving conditions (Figure 4.3b).
Interestingly no significant difference in cell survival was discerned in media containing either M-CSF or staurosporine (Figure 4.3).

It has been shown that Rictor deletion causes a cell cycle arrest in a variety of cell types [18, 50, 58]. In order to synchronize the cells we serum starved them for 24 hours to arrest the cells in G0/G1 and restimulated them with M-CSF (100ng/mL). In line with our expectations we found a distinct lag in G1 to S phase transition in both Rictor$^{\Delta M}$ BMDM and peritoneal macrophages (Figures 4.4 & 4.5). The overall low amount of 2-3% S-phase cells in peritoneal macrophages could be attributed to their function as mostly resident macrophages and a proliferative

burst only occurs post infection [9].
Furthermore we were able to identify low amounts of phosphorylated, and thus inactivated, cell cycle repressor Rb and more abundance of the cycline dependent kinase inhibitor p27(KIP1) as a possible reason for the lag in cell cycle progression from G1 to S phase in Rictor$^{\Delta M}$ macrophages (Figure 4.6) due to the lack of Akt-mediated phosphorylation of both former proteins. The experiment should be repeated with control macrophages treated with an Akt inhibitor in order to determine if lack of Akt-mediated phosphorylation of Rb and p27 is the sole cause for the observed delay in cell cycle progression.

Depending on environmental stimuli macrophages are able to polarize towards either an inflammatory M1 or tissue repairing M2 phenotype. That loss of mTORC2 function leads to a hyperinflammatory phenotype due to accumulation of FoxO1 in the nucleus upon LPS stimulation has been previously shown in MEFs and dendritic cells [34]. Preliminary experiments (Figure 4.7) in our group confirmed the hyperinflammatory phenotype in Rictor$^{\Delta M}$ bone marrow-derived macrophages.
Previous studies have reported that M1-polarized macrophages rely heavily on glycolysis as a means for ATP generation [10] and that overexpression of glucose transporter 1 (GLUT1) in macrophages leads to increased glucose uptake and secretion of inflammatory mediators [54], which could be reversed by the glycolytic inhibitor 2-DG. Another group recently highlighted that mTORC2 is of vital importance for an effective transfer of GLUT1 to the cell membrane [40].
With this in mind we used 2-NBDG as a fluorescent glucose analogue to measure the glucose uptake of unstimulated, LPS or IL-4 stimulated Rictor$^{\Delta M}$ and control BMDMs. We found that upon LPS stimulation the glucose uptake of Rictor$^{\Delta M}$ BMDMs was significantly lower and interestingly also after IL-4 stimulation (Figure 4.8).
We concluded that increased glycolytic metabolism could not be the reason for the hyperinflammatory phenotype of Rictor$^{\Delta M}$ macrophages and hypothesized that instead a dysfunctional mTORC2 inhibits M2 polarization.
To test this and also if diminished glycolytic metabolism negatively impacts M2 polarization, we stimulated Rictor$^{\Delta M}$ and control macrophages with IL-4 and the glycolytic inhibitor 2-DG.
Interestingly 2-DG was able to suppress the transcription of M2 marker gene Arg1 in control macrophages to a similar extent as observed in non 2-DG treated Rictor$^{\Delta M}$ macrophages (Figure 4.9), which suggests that glucose uptake and consequently glycolysis is also an important enabler of M2 polarization.

While M1 macrophages primarily make use of glycolysis for energy production, M2-polarized macrophages depend heavily on mitochondrial respiration and fatty acid oxidation. Through flow cytometry we assessed the mitochondrial mass and $\Delta\Psi$ as an indicator for OXPHOS, as $\Delta\Psi$, together with the proton gradient, form a transmembrane potential of H^+ ions that provides energy to the ATP synthase to produce ATP [59]. Recent studies reported a growth factor dependent localization of mTORC2 to the MAM complex and placed mTORC2 at the center of the MAM signaling hub [21]. The MAM is responsible for lipid and calcium transfer between the ER and mitochondria [60, 61] and its formation is regulated through various signal inputs, whereas the controlling mechanisms remain elusive.
Contrary to previous reports [21], conducted with Rictor knock out HeLa cells and MEFs, we found that in BMDM loss of Rictor leads to a significantly lower $\Delta\Psi$ and that incubation with the intracellular calcium releaser thapsigargin resulted in diminished $\Delta\Psi$ in control macrophages, whereas $\Delta\Psi$ levels in Rictor$^{\Delta M}$ remained unaffected. In contrast no differences in mitochondrial mass were found in either unstimulated or thapsigargin stimulated Rictor$^{\Delta M}$ BMDM (Figure 4.10).
These results show that $\Delta\Psi$ is negatively affected by, thapsigargin induced, constant Ca^{2+} release into the cytosol and Rictor deletion mimics this condition.
Also in case of the Rictor$^{\Delta M}$ macrophages that may be another explanation for the hyperinflammatory phenotype, because previous observations showed that upon LPS stimulation, increased intracellular Ca^{2+} leads to enhanced TNFα expression in macrophages [62].
Our data is in line with the results from Huang et al. who independently arrived at the same conclusion that mTORC2 plays a pivotal role in M2 polarization by managing glucose uptake [63], albeit they used extracellular acidification rate (ECAR) and glycolytic reserve (GR) to measure glycolytic activity and, instead of $\Delta\Psi$, utilized the O_2 consumption rate (OCR) and mitochondrial spare respiratory capacity (SRC) as an indicator for OXPHOS. Furthermore, data from Huang et al. suggested that the IL-4/Stat6 pathway runs parallel to M-CSF/mTORC2 in order to enhance IRF4 expression, which is an important transcription factor for glycolysis related genes.
Nevertheless further experiments should be done to solidify our findings and enhance our understanding of the mechanistic processes through which mTORC2 coordinates glucose uptake, mitochondrial respiration and ultimately M2 polarization. These could include live cell imaging of intracellular Ca^{2+} flux, mTOR and Rictor localization under various stimuli and gene set enrichment analysis.

As thapsigargin is also an inducer of ER stress and ER stress in BMDM potentiates the expression of inflammatory cytokines IL-6, TNFα and IL-1α upon TLR stimulation [47, 64], we investigated the abundance of ER stress markers GRP78 and GADD153/CHOP.

In line with our expectations we found elevated protein levels of GRP78 and GADD153/CHOP in both bone marrow-derived and peritoneal Rictor$^{\Delta M}$ macrophages, which might be caused by disrupted mitochondrial homeostasis and thus its inability to alleviate ongoing ER stress (Figure 4.11).

TLR signaling induces ER stress in macrophages and in turn augments the cellular response. Furthermore, the different pathways of the unfolded protein response are tightly regulated in concert with innate immune function [64]. Thus for further investigation of the impact of mTORC2 on ER stress alleviation in macrophages, we would recommend testing the long term impact of the elevated ER stress markers in unstimulated, IL-4 and TLR-ligand challenged Rictor$^{\Delta M}$ macrophages at various time points via qualitative and quantitative qPCR analysis, western blot and survival assays [65].

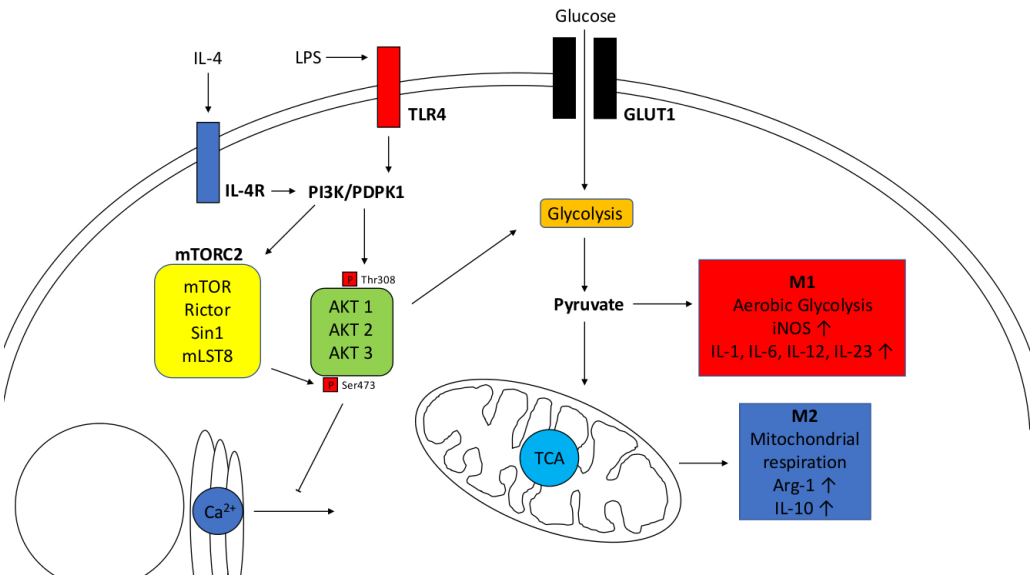

Figure 5.1: mTORC2 is nurturing glycolysis through Akt induced enhanced expression of different glycolytic enzymes and promotion of GLUT1 transfer to the cell membrane [40, 66, 67]. The glycolytic end product pyruvate can further be used for energy production in either aerobic glycolysis or mitochondrial respiration and our data suggests that a continuous glycolysis is required to supply enough pyruvate to the mitochondria for M2 polarization. Moreover mTORC2 stabilizes the MAM complex and inhibits unintended Ca^{2+} leakage from the ER into the cytosol.

In summary the primary findings of our work show that mTORC2 controls M2 polarization in macrophages by coordinating glycolysis and mitochondrial respira-

tion. Deletion of Rictor leads to diminished glucose uptake and M2 polarization in macrophages. Moreover, we could also reduce M2 polarization in control macrophages by inhibiting glycolysis via 2-DG and that is interesting because glycolysis is commonly associated as energy source for M1 polarization.

M2 polarization classically depends on mitochondrial respiration for energy and in line with that, upon loss of mTORC2 function we encountered decreased $\Delta\Psi$. Consequently our data hints that glycolysis might be important to nourish mitochondrial respiration for sustained M2 polarization.

As mTORC2 is also located at the MAM complex signaling hub, we found that disrupted calcium flux between ER and mitochondria could be another explanation for the abated $\Delta\Psi$, because, similar to lack of mTORC2, stimulation of control macrophages with the intracellular calcium releaser thapsigargin lowered their $\Delta\Psi$. These discoveries provide new insights into macrophage polarization and could be important for new treatments of M2 associated airway diseases and allergy.

References

[1] Jules Hoffmann and Shizuo Akira. "Innate immunity". In: *Current Opinion in Immunology* 25.1 (Feb. 2013), pp. 1–3. ISSN: 1879-0372. DOI: 10.1016/j.coi.2013.01.008.

[2] David Sancho and Caetano Reis e Sousa. "Sensing of cell death by myeloid C-type lectin receptors". In: *Current Opinion in Immunology* 25.1 (2013), pp. 46–52. ISSN: 0952-7915. URL: http://www.sciencedirect.com/science/article/pii/S0952791512001975.

[3] Himanshu Kumar, Taro Kawai, and Shizuo Akira. "Pathogen recognition by the innate immune system". In: *International Reviews of Immunology* 30.1 (Feb. 2011), pp. 16–34. ISSN: 1563-5244. DOI: 10.3109/08830185.2010.529976.

[4] David C. Dale, Laurence Boxer, and W. Conrad Liles. "The phagocytes: neutrophils and monocytes". In: *Blood* 112.4 (Aug. 15, 2008), pp. 935–945. ISSN: 0006-4971, 1528-0020. DOI: 10.1182/blood-2007-12-077917. URL: http://www.bloodjournal.org/content/112/4/935 (visited on 03/20/2017).

[5] Philip J. Vernon and Daolin Tang. "Eat-me: autophagy, phagocytosis, and reactive oxygen species signaling". In: *Antioxidants & Redox Signaling* 18.6 (Feb. 20, 2013), pp. 677–691. ISSN: 1557-7716. DOI: 10.1089/ars.2012.4810.

[6] Sakeen W. Kashem, Muzlifah Haniffa, and Daniel H. Kaplan. "Antigen-Presenting Cells in the Skin". In: *Annual Review of Immunology* (Feb. 6, 2017). ISSN: 1545-3278. DOI: 10.1146/annurev-immunol-051116-052215.

[7] Priyanka Nair-Gupta et al. "TLR Signals Induce Phagosomal MHC-I Delivery from the Endosomal Recycling Compartment to Allow Cross-Presentation". In: *Cell* 158.3 (July 31, 2014), pp. 506–521. ISSN: 0092-8674. DOI: 10.1016/j.cell.2014.04.054. URL: http://www.ncbi.nlm.nih.gov/pmc/articles/PMC4212008/ (visited on 03/30/2017).

[8] Emmanuel L. Gautier et al. "Gene expression profiles and transcriptional regulatory pathways underlying mouse tissue macrophage identity and diversity". In: *Nature immunology* 13.11 (Nov. 2012), pp. 1118–1128. ISSN: 1529-2908. DOI: 10.1038/ni.2419. URL: http://www.ncbi.nlm.nih.gov/pmc/articles/PMC3558276/ (visited on 04/06/2017).

[9] Luke C. Davies et al. "A quantifiable proliferative burst of tissue macrophages restores homeostatic macrophage populations after acute inflammation". In: *European Journal of Immunology* 41.8 (Aug. 2011), pp. 2155–2164. ISSN: 1521-4141. DOI: 10.1002/eji.201141817.

[10] Erika L. Pearce and Edward J. Pearce. "Metabolic Pathways In Immune Cell Activation And Quiescence". In: *Immunity* 38.4 (Apr. 18, 2013), pp. 633–643. ISSN: 1074-7613. DOI: 10.1016/j.immuni.2013.04.005. URL: http://www.ncbi.nlm.nih.gov/pmc/articles/PMC3654249/ (visited on 11/03/2016).

[11] Paola Italiani and Diana Boraschi. "From Monocytes to M1/M2 Macrophages: Phenotypical vs. Functional Differentiation". In: *Frontiers in Immunology* 5 (Oct. 17, 2014). ISSN: 1664-3224. DOI: 10.3389/fimmu.2014.00514. URL: http://www.ncbi.nlm.nih.gov/pmc/articles/PMC4201108/ (visited on 11/03/2016).

[12] Guillermo Arango Duque and Albert Descoteaux. "Macrophage Cytokines: Involvement in Immunity and Infectious Diseases". In: *Frontiers in Immunology* 5 (2014). ISSN: 1664-3224. DOI: 10.3389/fimmu.2014.00491. URL: https://www.frontiersin.org/articles/10.3389/fimmu.2014.00491/full (visited on 11/07/2017).

[13] Ling Zhang and Cheng-Cai Wang. "Inflammatory response of macrophages in infection". In: *Hepatobiliary & pancreatic diseases international: HBPD INT* 13.2 (Apr. 2014), pp. 138–152. ISSN: 1499-3872.

[14] Beth Kelly and Luke AJ O'Neill. "Metabolic reprogramming in macrophages and dendritic cells in innate immunity". In: *Cell Research* 25.7 (July 2015), pp. 771–784. ISSN: 1001-0602. DOI: 10.1038/cr.2015.68. URL: http://www.nature.com/cr/journal/v25/n7/full/cr201568a.html (visited on 05/19/2016).

[15] Stephan Wullschleger, Robbie Loewith, and Michael N. Hall. "{TOR} Signaling in Growth and Metabolism". In: *Cell* 124.3 (2006), pp. 471–484. ISSN: 0092-8674. DOI: http://dx.doi.org/10.1016/j.cell.2006.01.016. URL: http://www.sciencedirect.com/science/article/pii/S0092867406001085.

[16] Mathieu Laplante and David M. Sabatini. "mTOR signaling at a glance". In: *Journal of Cell Science* 122.20 (2009), pp. 3589–3594. ISSN: 0021-9533. DOI: 10.1242/jcs.051011. eprint: http://jcs.biologists.org/content/122/20/3589.full.pdf. URL: http://jcs.biologists.org/content/122/20/3589.

[17] Thomas Weichhart, Markus Hengstschläger, and Monika Linke. "Regulation of innate immune cell function by mTOR". In: *Nature Reviews. Immunology* 15.10 (Oct. 2015), pp. 599–614. ISSN: 1474-1741. DOI: 10.1038/nri3901.

[18] Margit Rosner and Markus Hengstschläger. "Cytoplasmic and nuclear distribution of the protein complexes mTORC1 and mTORC2: rapamycin triggers dephosphorylation and delocalization of the mTORC2 components rictor and sin1". In: *Human Molecular Genetics* 17.19 (2008), pp. 2934–2948. DOI: 10.1093/hmg/ddn192. eprint: http://hmg.oxfordjournals.org/content/17/19/2934.full.pdf+html. URL: http://hmg.oxfordjournals.org/content/17/19/2934.abstract.

[19] Margit Rosner and Markus Hengstschläger. "mTOR protein localization is cell cycle-regulated". In: *Cell Cycle* 10.20 (Oct. 2011), pp. 3608–3610. ISSN: 1538-4101. DOI: 10.4161/cc.10.20.17855. URL: https://doi.org/10.4161/cc.10.20.17855.

[20] Charles Betz and Michael N. Hall. "Where is mTOR and what is it doing there?" In: *The Journal of Cell Biology* 203.4 (2013), pp. 563–574. DOI: 10.1083/jcb.201306041. eprint: http://jcb.rupress.org/content/203/4/563.full.pdf+html. URL: http://jcb.rupress.org/content/203/4/563.abstract.

[21] Charles Betz et al. "Feature Article: mTOR complex 2-Akt signaling at mitochondria-associated endoplasmic reticulum membranes (MAM) regulates mitochondrial physiology". In: *Proceedings of the National Academy of Sciences of the United States of America* 110.31 (July 30, 2013), pp. 12526–12534. ISSN: 1091-6490. DOI: 10.1073/pnas.1302455110.

[22] Pengda Liu et al. "PtdIns(3,4,5)P(3)-dependent Activation of the mTORC2 Kinase Complex". In: *Cancer discovery* 5.11 (Aug. 2015), pp. 1194–1209. ISSN: 2159-8290. URL: http://www.ncbi.nlm.nih.gov/pmc/articles/PMC4631654/.

[23] Shunsuke Mori et al. "The mTOR Pathway Controls Cell Proliferation by Regulating the FoxO3a Transcription Factor via SGK1 Kinase". In: *PLoS ONE* 9.2 (Jan. 2014), e88891. ISSN: 1932-6203. URL: http://www.ncbi.nlm.nih.gov/pmc/articles/PMC3928304/.

[24] Dos D. Sarbassov et al. "Rictor, a Novel Binding Partner of mTOR, Defines a Rapamycin-Insensitive and Raptor-Independent Pathway that Regulates the Cytoskeleton". In: *Current Biology* 14.14 (), pp. 1296–1302. ISSN: 0960-9822. DOI: 10.1016/j.cub.2004.06.054. URL: http://dx.doi.org/10.1016/j.cub.2004.06.054.

[25] Lunhua Liu et al. "mTORC2 regulates neutrophil chemotaxis in a cAMP- and RhoA-dependent fashion". In: *Developmental Cell* 19.6 (Dec. 14, 2010), pp. 845–857. ISSN: 1878-1551. DOI: 10.1016/j.devcel.2010.11.004.

[26] Lunhua Liu and Carole A. Parent. "TOR kinase complexes and cell migration". In: *J Cell Biol* 194.6 (Sept. 2011), p. 815. URL: http://jcb.rupress.org/content/194/6/815.abstract.

[27] Kenta Masui et al. "mTOR complex 2 controls glycolytic metabolism in glioblastoma through FoxO acetylation and upregulation of c-Myc". In: *Cell Metabolism* 18.5 (Nov. 5, 2013), pp. 726–739. ISSN: 1932-7420. DOI: 10.1016/j.cmet.2013.09.013.

[28] Kenta Masui et al. "Glucose-dependent acetylation of Rictor promotes targeted cancer therapy resistance". In: *Proceedings of the National Academy of Sciences of the United States of America* 112.30 (July 2015), pp. 9406–9411. ISSN: 1091-6490. URL: http://www.ncbi.nlm.nih.gov/pmc/articles/PMC4522814/.

[29] Chiyo Shiota et al. "Multiallelic Disruption of the ¡em¿rictor¡/em¿ Gene in Mice Reveals that mTOR Complex 2 Is Essential for Fetal Growth and Viability". In: *Developmental Cell* 11.4 (), pp. 583–589. ISSN: 1534-5807. DOI: 10.1016/j.devcel.2006.08.013. URL: http://dx.doi.org/10.1016/j.devcel.2006.08.013.

[30] Ralf Kühn and Raul M. Torres. "Cre/loxP Recombination System and Gene Targeting". In: *Transgenesis Techniques: Principles and Protocols*. Totowa, NJ: Springer New York, 2002, pp. 175–204. URL: https://doi.org/10.1385/1-59259-178-7:175.

[31] B. Möllers et al. "The mouse M-lysozyme gene domain: identification of myeloid and differentiation specific DNasel hypersensitive sites and of a 3'-cis acting regulatory element." In: *Nucleic Acids Research* 20.8 (Apr. 1992), pp. 1917–1924. ISSN: 1362-4962. URL: http://www.ncbi.nlm.nih.gov/pmc/articles/PMC312307/.

[32] B. E. Clausen et al. "Conditional gene targeting in macrophages and granulocytes using LysMcre mice". In: *Transgenic Research* 8.4 (1999), pp. 265–277. ISSN: 1573-9368. URL: https://doi.org/10.1023/A:1008942828960.

[33] Taro Fukao and Shigeo Koyasu. "PI3K and negative regulation of TLR signaling". In: *Trends in Immunology* 24.7 (July 1, 2003), pp. 358–363. ISSN: 1471-4906, 1471-4981. DOI: 10.1016/S1471-4906(03)00139-X. URL: /trends/immunology/abstract/S1471-4906(03)00139-X (visited on 09/07/2016).

[34] Jonathan Brown et al. "Mammalian target of rapamycin complex 2 (mTORC2) negatively regulates Toll-like receptor 4-mediated inflammatory response via FoxO1". In: *The Journal of Biological Chemistry* 286.52 (Dec. 30, 2011), pp. 44295–44305. ISSN: 1083-351X. DOI: 10.1074/jbc.M111.258053.

[35] William T. Festuccia et al. "Myeloid-specific Rictor deletion induces M1 macrophage polarization and potentiates in vivo pro-inflammatory response to lipopolysaccharide". In: *PloS One* 9.4 (2014), e95432. ISSN: 1932-6203. DOI: 10.1371/journal.pone.0095432.

[36] Karl Katholnig et al. "Immune responses of macrophages and dendritic cells regulated by mTOR signalling". In: *Biochemical Society Transactions* 41.4 (Aug. 2013), pp. 927–933. ISSN: 1470-8752. DOI: 10.1042/BST20130032.

[37] Johannes Schindelin et al. "Fiji: an open-source platform for biological-image analysis". In: *Nature Methods* 9.7 (July 2012), pp. 676–682. ISSN: 1548-7105. DOI: 10.1038/nmeth.2019.

[38] Frederick A. Dick and Seth M. Rubin. "Molecular mechanisms underlying RB protein function". In: *Nature reviews. Molecular cell biology* 14.5 (May 2013), pp. 297–306. ISSN: 1471-0072. DOI: 10.1038/nrm3567. URL: http://www.ncbi.nlm.nih.gov/pmc/articles/PMC4754300/ (visited on 11/03/2016).

[39] Incheol Shin et al. "PKB/Akt mediates cell-cycle progression by phosphorylation of p27(Kip1) at threonine 157 and modulation of its cellular localization". In: *Nature Medicine* 8.10 (Oct. 2002), pp. 1145–1152. ISSN: 1078-8956. DOI: 10.1038/nm759.

[40] Jessica M. Olsen et al. "Glucose uptake in brown fat cells is dependent on mTOR complex 2-promoted GLUT1 translocation". In: *The Journal of Cell Biology* 207.3 (Nov. 10, 2014), pp. 365–374. ISSN: 1540-8140. DOI: 10.1083/jcb.201403080.

[41] H. M. Shapiro. "Membrane potential estimation by flow cytometry". In: *Methods (San Diego, Calif.)* 21.3 (July 2000), pp. 271–279. ISSN: 1046-2023. DOI: 10.1006/meth.2000.1007.

[42] Eva Kmonícková et al. "Modulator of intracellular Ca(2+), thapsigargin, interferes with in vitro secretion of cytokines and nitric oxide". In: *Biomedical Papers of the Medical Faculty of the University Palacký, Olomouc, Czechoslovakia* 149.2 (Dec. 2005), pp. 321–324. ISSN: 1213-8118.

[43] Paavo Korge and James N. Weiss. "Thapsigargin directly induces the mitochondrial permeability transition". In: *European Journal of Biochemistry* 265.1 (Oct. 1999), pp. 273–280. ISSN: 1432-1033. URL: http://dx.doi.org/10.1046/j.1432-1327.1999.00724.x.

[44] B. Wright et al. "Inhibition of macrophage activation by calcium channel blockers and calmodulin antagonists". In: *Cellular Immunology* 95.1 (Oct. 1, 1985), pp. 46–53. ISSN: 0008-8749. DOI: 10.1016/0008-8749(85)90293-X. URL: http://www.sciencedirect.com/science/article/pii/000887498590293X (visited on 05/17/2016).

[45] Ling Zeng et al. "XBP-1 couples endoplasmic reticulum stress to augmented IFN-β induction via a cis-acting enhancer in macrophages". In: *Journal of immunology (Baltimore, Md. : 1950)* 185.4 (July 2010), pp. 2324–2330. ISSN: 1550-6606. URL: http://www.ncbi.nlm.nih.gov/pmc/articles/PMC2916979/.

[46] Yi-Ping Liu et al. "Endoplasmic reticulum stress regulates the innate immunity critical transcription factor IRF3". In: *Journal of Immunology (Baltimore, Md.: 1950)* 189.9 (Nov. 1, 2012), pp. 4630–4639. ISSN: 1550-6606. DOI: 10.4049/jimmunol.1102737.

[47] Chenyang Zhao et al. "Cellular stress amplifies TLR3/4 induced CXCL1/2 gene transcription in mononuclear phagocytes via RIPK1". In: *Journal of immunology (Baltimore, Md. : 1950)* 193.2 (June 2014), pp. 879–888. ISSN: 1550-6606. URL: http://www.ncbi.nlm.nih.gov/pmc/articles/PMC4091718/.

[48] K. L. Bost and M. J. Mason. "Thapsigargin and cyclopiazonic acid initiate rapid and dramatic increases of IL-6 mRNA expression and IL-6 secretion in murine peritoneal macrophages." In: *J. Immunol.* 155.1 (July 1995), p. 285. URL: http://www.jimmunol.org/content/155/1/285.abstract.

[49] Margit Rosner et al. "Functional interaction of mammalian target of rapamycin complexes in regulating mammalian cell size and cell cycle". In: *Human Molecular Genetics* 18.17 (Sept. 1, 2009), pp. 3298–3310. ISSN: 1460-2083. DOI: 10.1093/hmg/ddp271.

[50] Craig R. Stumpf et al. "The translational landscape of the mammalian cell cycle". In: *Molecular Cell* 52.4 (Nov. 21, 2013), pp. 574–582. ISSN: 1097-4164. DOI: 10.1016/j.molcel.2013.09.018.

[51] Liqun Zhao et al. "mTOR complex 2 is involved in regulation of Cbl-dependent c-FLIP degradation and sensitivity of TRAIL-induced apoptosis". In: *Cancer Research* 73.6 (Mar. 15, 2013), pp. 1946–1957. ISSN: 1538-7445. DOI: 10.1158/0008-5472.CAN-12-3710.

[52] Priyajit Chatterjee et al. "A carbazole alkaloid deactivates mTOR through the suppression of rictor and that induces apoptosis in lung cancer cells". In: *Molecular and Cellular Biochemistry* 405.1 (2015), pp. 149–158. ISSN: 1573-4919. URL: https://doi.org/10.1007/s11010-015-2406-2.

[53] Yu-Hai Bian et al. "Targeting mTORC2 component rictor inhibits cell proliferation and promotes apoptosis in gastric cancer". In: *American Journal of Translational Research* 9.9 (Aug. 2017), pp. 4317–4330. ISSN: 1943-8141. URL: http://www.ncbi.nlm.nih.gov/pmc/articles/PMC5622274/.

[54] Alex J. Freemerman et al. "Metabolic Reprogramming of Macrophages". In: *The Journal of Biological Chemistry* 289.11 (Mar. 14, 2014), pp. 7884–7896. ISSN: 0021-9258. DOI: 10.1074/jbc.M113.522037. URL: http://www.ncbi.nlm.nih.gov/pmc/articles/PMC3953299/ (visited on 05/19/2016).

[55] Won Jun Oh and Estela Jacinto. "mTOR complex 2 signaling and functions". In: *Cell Cycle (Georgetown, Tex.)* 10.14 (July 15, 2011), pp. 2305–2316. ISSN: 1551-4005. DOI: 10.4161/cc.10.14.16586.

[56] Fei Zhang et al. "mTOR complex component Rictor interacts with PKCzeta and regulates cancer cell metastasis." eng. In: *Cancer Res* 70.22 (Nov. 2010), pp. 9360–9370. DOI: 10.1158/0008-5472.CAN-10-0207. URL: http://dx.doi.org/10.1158/0008-5472.CAN-10-0207.

[57] Dmitry Namgaladze, Andreas Kollas, and Bernhard Brüne. "Oxidized LDL attenuates apoptosis in monocytic cells by activating ERK signaling". In: *Journal of Lipid Research* 49.1 (Jan. 2008), pp. 58–65. ISSN: 0022-2275. DOI: 10.1194/jlr.M700100-JLR200.

[58] Daniel Smrz et al. "mTORC1 and mTORC2 differentially regulate homeostasis of neoplastic and non-neoplastic human mast cells". In: *Blood* 118.26 (Dec. 22, 2011), pp. 6803–6813. ISSN: 1528-0020. DOI: 10.1182/blood-2011-06-359984.

[59] Ljubava D. Zorova et al. "Mitochondrial membrane potential". In: *Analytical Biochemistry* (2017). ISSN: 0003-2697. URL: http://www.sciencedirect.com/science/article/pii/S0003269717302932.

[60] Rosario Rizzuto et al. "Close Contacts with the Endoplasmic Reticulum as Determinants of Mitochondrial Ca²⁺ Responses". In: *Science* 280.5370 (June 1998), p. 1763. URL: http://science.sciencemag.org/content/280/5370/1763.abstract.

[61] G. Csordás, A. P. Thomas, and G. Hajnóczky. "Quasi-synaptic calcium signal transmission between endoplasmic reticulum and mitochondria." In: *The EMBO Journal* 18.1 (Jan. 1999), pp. 96–108. ISSN: 1460-2075. URL: http://www.ncbi.nlm.nih.gov/pmc/articles/PMC1171106/.

[62] Naoko Watanabe, Junko Suzuki, and Yoshiro Kobayashi. "Role of Calcium in Tumor Necrosis Factor-α Production by Activated Macrophages:" in: *The Journal of Biochemistry* 120.6 (1996), pp. 1190–1195.

[63] Stanley Ching-Cheng Huang et al. "mTORC2-IRF4 mediated metabolic reprograming is essential for macrophage alternative activation". In: *Immunity* 45.4 (Oct. 2016), pp. 817–830. ISSN: 1097-4180. URL: http://www.ncbi.nlm.nih.gov/pmc/articles/PMC5535820/.

[64] Fabio Martinon et al. "Toll-like receptor activation of XBP1 regulates innate immune responses in macrophages". In: *Nature immunology* 11.5 (Mar. 2010), pp. 411–418. ISSN: 1529-2916. URL: http://www.ncbi.nlm.nih.gov/pmc/articles/PMC3113706/.

[65] Donna Kennedy, Afshin Samali, and Richard Jäger. "Methods for Studying ER Stress and UPR Markers in Human Cells". In: *Stress Responses: Methods and Protocols*. New York, NY: Springer New York, 2015, pp. 3–18. URL: https://doi.org/10.1007/978-1-4939-2522-3_1.

[66] Kenta Masui, Webster K. Cavenee, and Paul S. Mischel. "mTORC2 in the center of cancer metabolic reprogramming". In: *Trends in endocrinology and metabolism: TEM* 25.7 (May 2014), pp. 364–373. ISSN: 1879-3061. URL: http://www.ncbi.nlm.nih.gov/pmc/articles/PMC4077930/.

[67] Asami Hagiwara et al. "Hepatic mTORC2 activates glycolysis and lipogenesis through Akt, glucokinase, and SREBP1c". In: *Cell Metabolism* 15.5 (May 2, 2012), pp. 725–738. ISSN: 1932-7420. DOI: 10.1016/j.cmet.2012.03.015.